Final Report

DE-FG02-03CH11171

" PowerGrid - A Computation Engine for Large-Scale Electric Networks"

Submitted to

Department of Energy

Prepared by

C.O. Nwankpa
Center for Electric Power Engineering
Drexel University
32nd and Chestnut Streets
Philadelphia, PA. 19104

December 2010

TABLE OF CONTENTS

LIST OF TABLES

LIST OF FIGURES

ABSTRACT

This Final Report discusses work on an approach for analog emulation of large scale power systems using Analog Behavioral Models (ABMs) and analog devices in PSpice design environment. ABMs are models based on sets of mathematical equations or transfer functions describing the behavior of a circuit element or an analog building block. The ABM concept provides an efficient strategy for feasibility analysis, quick insight of developing top-down design methodology of large systems and model verification prior to full structural design and implementation. Analog emulation in this report uses an electric circuit equivalent of mathematical equations and scaled relationships that describe the states and behavior of a real power system to create its solution trajectory. The speed of analog solutions is as quick as the responses of the circuit itself. Emulation therefore is the representation of desired physical characteristics of a real life object using an electric circuit equivalent. The circuit equivalent has within it, the model of a real system as well as the method of solution. This report presents a methodology of the core computation through development of ABMs for generators, transmission lines and loads. Results of ABMs used for the case of 3, 6, and 14 bus power systems are presented and compared with industrial grade numerical simulators for validation.

1. INTRODUCTION

1.1 OVERVIEW

This report explores the feasibility of implementation of analog emulation of large-scale power systems using ABMs and analog devices in PSpice design environment. The end goal is to develop a very fast, programmable, and reconfigurable power system emulator using analog/mixed signal VLSI chip. The said VLSI chip will house a very large scaled-down power system network that will be capable of emulating desired behaviors of real power systems under various conditions. Its computation is independent of size of the power network and can be controlled to be in real-time or faster than real-time.

This report discusses steps toward attaining this goal. The approach uses ABMs as building blocks to develop software simulation of an analog emulator that emulates the evaluation of states of a real power system. That is, solving the mathematical equations and scaled components that mimic power system behavior, ABMs and analog devices in PSpice circuit design environments are used to build modules of generator, transmission networks, and loads. The approach explores the analog natural characteristic of massively parallel collective computation of large number of signals that are continuous in time and amplitude. This characteristic gives an edge over digital simulators in terms of computation time. A simplified illustration of developmental stages to the end goal is described in Figure 1.1 below.

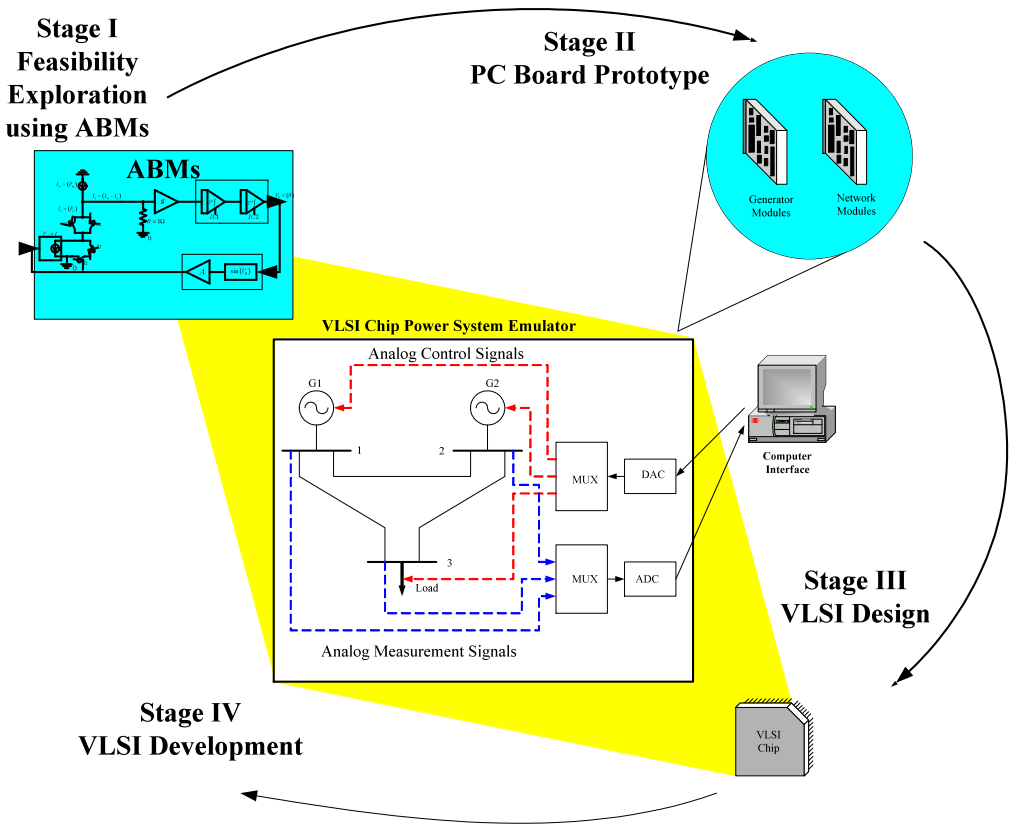

Figure 1.1: A Simplified Illustration of Developmental Stages to PSoC

The illustration consists of:

i) The end goal – a VLSI Chip Power System Emulator that houses a scaled-down power network, represented here as a three-bus system with communication and measurement channels for actuation and sensing;

ii) Stage I is the exploration of feasibility of emulator design and realization using ABMs and analog devices in PSpice environment; the verification and validation of power system core computation methodology and circuit layouts - the main focus of this report;

iii) Stage II is the Printed Circuit Board (PCB) design and realization of a small scale prototype for further testing and troubleshooting;

iv) Stage III is the actual VLSI design of a large scale prototype; and

v) Stage IV is the development and fabrication of the VLSI chip or Power System on a Chip (PSoC).

The ABM concept as used in this report offers further insight into intricacies of circuit connections, number of circuit elements/building blocks, types of inputs/outputs, etc.

Analog Behavioral Models (ABMs) are models based on sets of mathematical equations or transfer functions that describe the behavior of a circuit element or an analog building block. A behavioral model is similar to a subcircuit in that it constitutes an object which is connected to a circuit through electrical ports. The interior of a behavioral model however, is different in that it is implemented in terms of symbolic mathematical equations or transfer functions rather than a netlist [1,2]. The ABM concept provides an efficient strategy for feasibility studies and analysis, quick insights into developing top-down design methodology of large complex systems and model verification prior to full structural design and implementation.

1.2 ORGANIZATION OF REPORT

The next section gives a brief overview of the power network model, computation methodology, and analog emulator setup. Then, development of analog emulator modules using ABMs is described in detail. This is followed by section that presents the results of PSpice simulation runs on the proposed emulator and its validations. The conclusion of the report, summary of work and recommendation for future work is given in the final section.

2. METHODOLOGY AND DEVELOPMENT OF ANALOG EMULATOR

2.1 CORE COMPUTATION METHODOLOGY OVERVIEW

Power system core computation methodology as implemented in this report goes through three major steps:

Step 1: Calculating currents in the network

The complex current flowing in any branch or transmission line is as a result of interaction between the bus or node voltages and transmission line impedance and loads (if not lumped with line impedance).

Step II: Calculating generator electrical power

The electrical power out of each generator in the system is calculated as the real part of the product of the generator terminal voltage and complex conjugate of the generator current;

Step III: Swing Equation update and computing generator power angle

The swing equation describes the dynamics of a generator. Its input is a mechanical power from prime mover and which is assumed constant. The output of a generator is an electrical power, which changes in accordance with the state of the network. The swing equation is a second order differential equation and its solution is the power angle of the generator. The power angle combines with generator internal voltage to constantly update the generator terminal voltage and hence the generator current. Figure 3.7 describes the continuous cycle of power system core computation. Detail

computation methodology and implementation of each of the stages are further discussed in the next subsections.

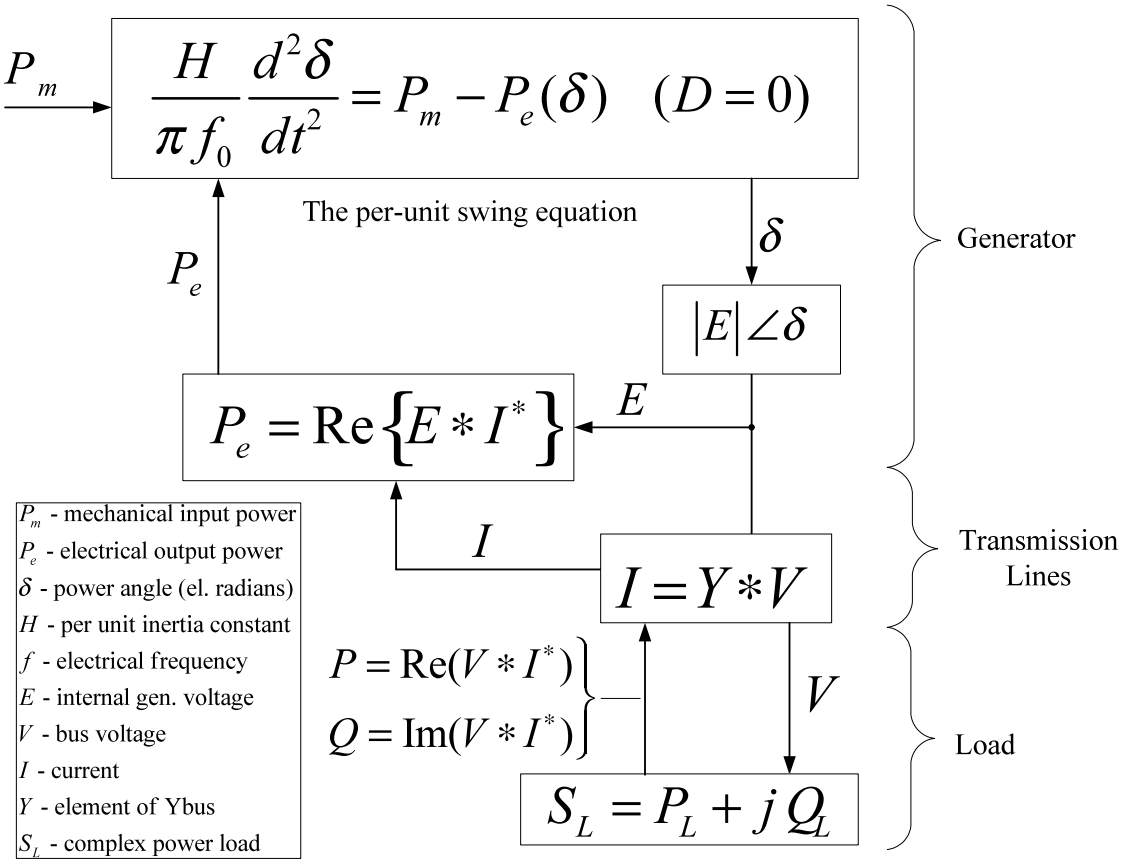

Figure 2.1: Block Diagram of Core Computation Methodology of Analog Emulator

2.2 COMPLEX CURRENT COMPUTATION METHODOLOGY AND IMPLEMENTATION

The complex current flowing in any branch or transmission line is as a result of interaction between the bus or node voltages and transmission line impedance. Using admittance for simplicity and expressed in rectangular form, we have;

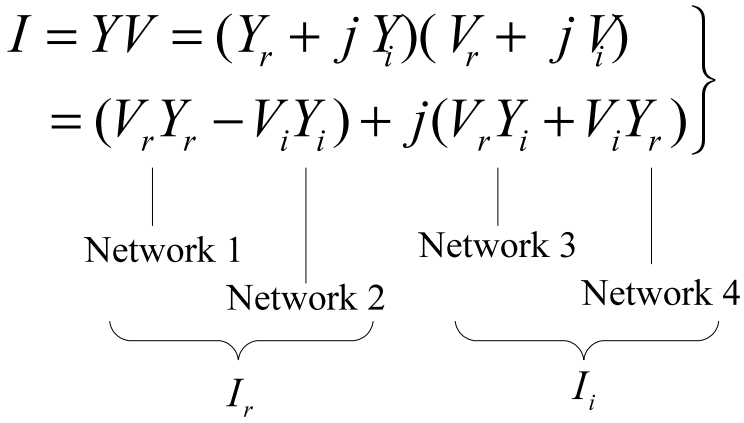

Figure 2.2: Complex Current Computation Methodology

where subscripts r and i represents real and imaginary part, respectively.

From Figure 2.2 above, it will require four separate networks in order to emulate the complex current flowing on any branch. Using the approach proposed by Fried et al [28], four separate dc-resistive networks can be used. The assumption is that changes in angular frequency in the system are very small (1-2%) and might be considered as constant ($\omega \approx \omega_0$=constant). Therefore the transmission network can be emulated using frequency independent programmable resistors built on Operational Transconductance Amplifiers (OTAs). The transformation of the transmission line complex impedance to its resistance value for the real and imaginary part is through complex conjugation as shown in equation (2.1):

$$\left.\begin{aligned} Y &= \frac{1}{Z} = \frac{1}{R + jX} = \frac{R - jX}{R^2 + X^2} \\ Y_{\text{Re}} &= \frac{R}{R^2 + X^2} = Y_r \\ Y_{\text{Im}} &= (-)\frac{X}{R^2 + X^2} = Y_i \end{aligned}\right\} \tag{2.1}$$

Combining equation (2.1) with Figure 2.1, we can show the implementation of complex current computation as described in Figure 2.2.

This means that the real part of complex current flowing through any branch is given by the sum of component currents in networks 1 and 2, and the imaginary part as the difference between component currents in networks 4 and 3, as summarized below.

$$\left.\begin{aligned} I &= I_r + jI_i \\ I_r &= I^{I} + I^{II} \\ I_i &= I^{IV} - I^{III} \end{aligned}\right\} \tag{2.2}$$

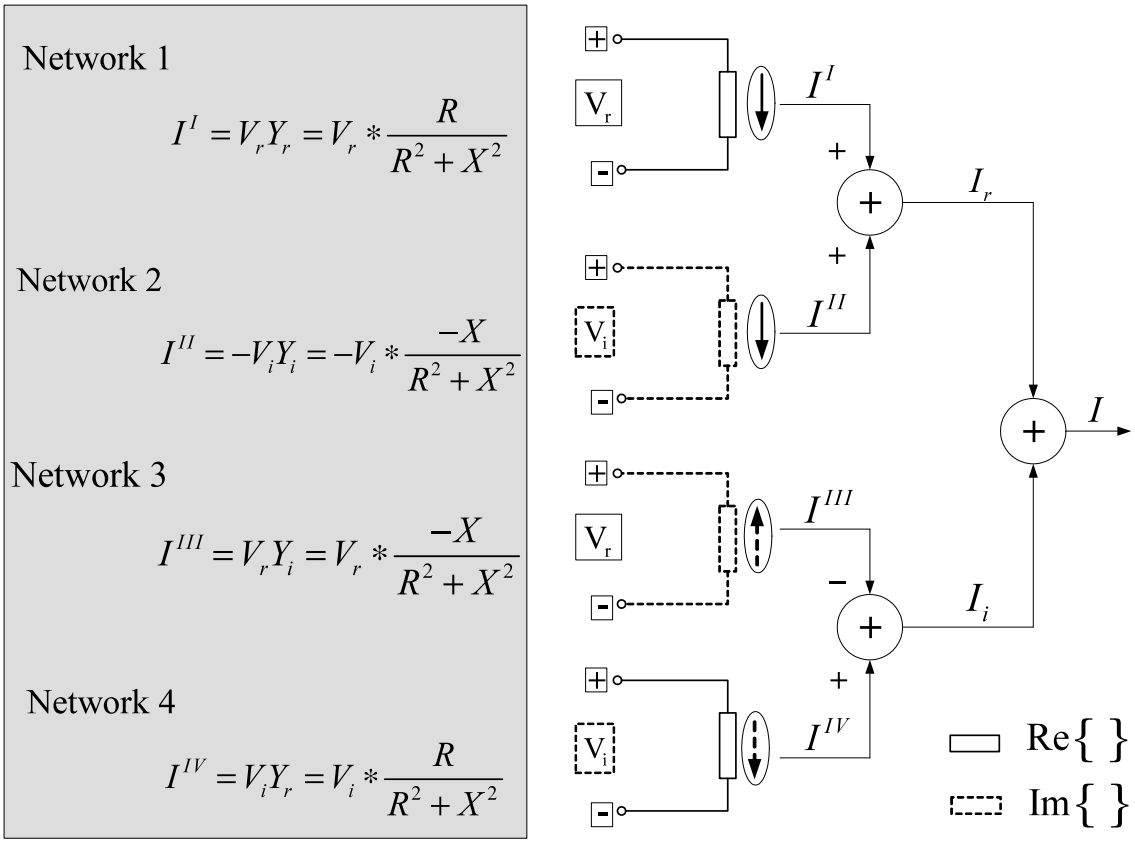

Figure 2.3: Complex Current Computation Implementation.

where

I is the complex current flowing through a branch.

I_r and I_i are real and imaginary parts of complex current flowing through a branch.

$I^I, I^{II}, I^{III},$ and I^{IV} are component currents flowing through a branch emulated as networks 1,2,3 and 4, respectively.

V_r and V_i are real and imaginary parts of bus complex voltage.

$Z = R + jX$ is line impedance with its resistance and reactance components.

Y is the line admittance.

2.3 REAL POWER COMPUTATION METHODOLOGY

The electrical power out of the generator is computed according to equation (2.3). Generator complex current is determined based on the principle described in section 2.2. Figure 2.4 illustrates electric power computation implementation.

$$P_{e_i} = \mathrm{Re}\{E_{g_i} * I_{g_i}^*\} = \mathrm{Re}\{E_{g_i}\} * \mathrm{Re}\{I_{g_i}\} + \mathrm{Im}\{E_{g_i}\} * \mathrm{Im}\{I_{g_i}\} \tag{2.3}$$

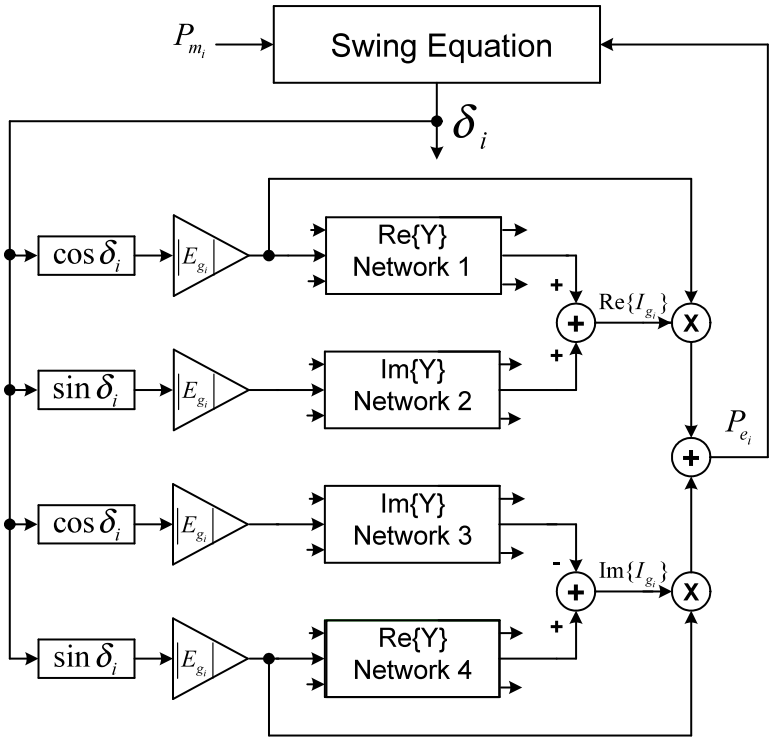

Figure 2.4: Generator Real Power Computation Methodology [28]

The real part of the product of generator voltage and complex conjugated current gives the generator electrical power. The electrical angle at time t_0 determines the electrical power at time t_{0+} through the change of the real and imaginary parts of the voltages in the four dc emulating networks.

2.4 COMPUTATIONALLY FEASIBLE BUS VOLTAGES

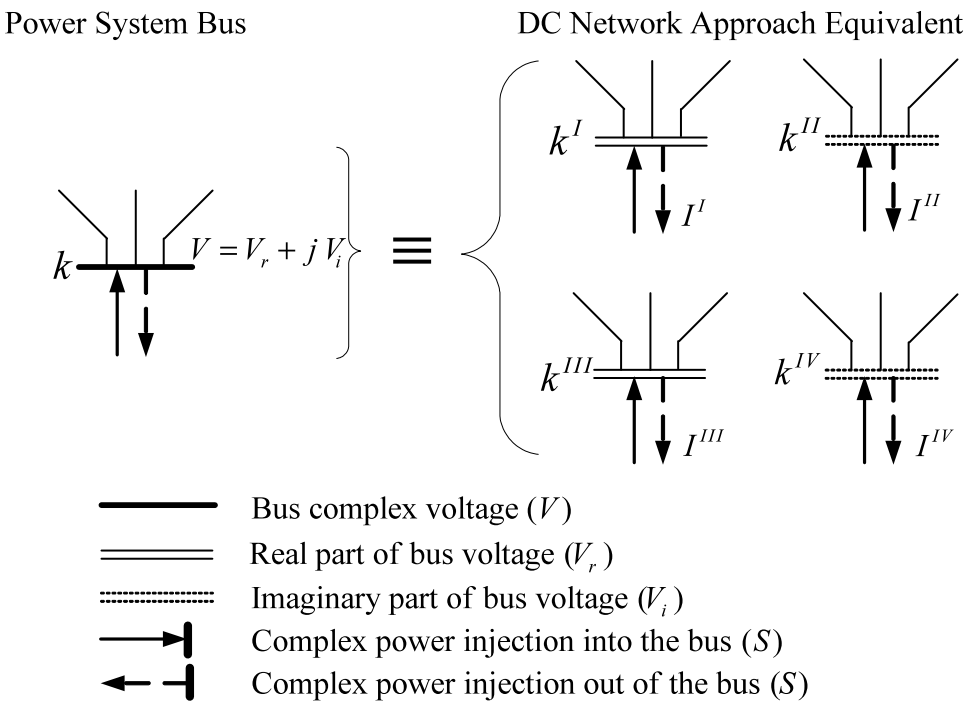

Figure 2.5: Computationally Feasible Bus Voltage

Figure 2.5 describes the dc-network equivalent of a real power system bus and conditions for its implementation. Analyzing a sample power system and considering an

arbitrary bus k with its complex voltage values, we have 4 networks with 4 buses: k^I, k^{II}, k^{III} and k^{IV} as equivalents. For feasible bus voltages, the following conditions must be satisfied:

$$\left.\begin{aligned} V_{k^I} &= V_{k^{III}} = V_{k_r} \\ V_{k^{II}} &= V_{k^{IV}} = V_{k_i} \end{aligned}\right\} \tag{2.4}$$

It is then and only then that the current computation methodology described in subsection 2.2 will yield accurate and feasible values. The feasible bus voltages condition is realizable as a result of the constant PQ-load model differential form discussed in subsections 2.2 and 2.6.3.

2.5 ANALOG EMULATOR SETUP

Analog emulation in other words may be described as an automatic means of representing the performance of a physical system by solving the mathematical equations or scaled relationships defining the behavior of the system in a continuous manner. The features that make the proposed scheme a viable option and an edge over digital or numerical simulator in solving power system problems are [31]:

i. The dynamic range of power system problems matches that of current analog circuitry;
ii. The nature and type of mathematical equations that describe the states and behaviors of power system under various conditions can be represented using

analog devices and analog building blocks (for example, integration, multiplication, summing, etc.);

iii. Power system variables that are complex in nature and are usually represented in phasor form can easily be converted and expressed in rectangular form (Cartesian Coordinate), the form that is more efficiently represented in analog circuits;

iv. The representation of a real power system on an analog emulator can be scaled both in time and amplitude. With proper choice of time-scale factor, the speed of analog computation of any size of power system can be made faster or slower than real-time. In addition, a large-scale power system can be mapped on a VLSI chip, using the appropriate magnitude-scaling factors for input and output variables. Evolution of VLSI technology has developed to the point where millions of electronic devices can be integrated on a single chip [27].

2.6 DEVELOPMENT OF ANALOG EMULATOR MODULES

The analog power system emulator proposed in this report is based on using analog devices to build electric circuit equivalents of mathematical equations and scaled relationship model representations of real power system states and behaviors under different circumstances. Separate modules will be built for generator, transmission network and load in subsections 2.6.1 through 2.6.3, respectively using power system models discussed in section 2.2 and elaborated on section 2.3. The methodology

described in section 2.4 in combination with setup approach of section 2.5 is the basis of the analog emulator implementation.

2.6.1 GENERATOR MODULE

A generator module is built using the classical model discussed in subsection 2.1. General purpose mathematical analogs built using ABMs are interconnected to emulate equations (3.1) and (3.2). Rewriting equation (3.1):

$$\left(\frac{H}{\pi f_0}\right)\left(\frac{d^2\delta}{dt^2}\right) = P_a = P_m - P_{\max}\sin\delta \quad \text{per unit}$$
$$\text{where} \quad P_e = P_{\max}\sin\delta; \tag{2.5}$$
$$\text{and } P_{\max} = \frac{\left|E'\right|\left|V\right|}{\left(X_d' + X_l\right)} \quad \text{for a lossless line.}$$

The following notations are used for the power system variables and parameters:

E' internal generator voltage
V bus voltage
X_l line reactance

The swing equation is a second order differential equation and a nonlinear function of the power angle. Rearranging equation (2.5) gives

$$\frac{d^2\delta}{dt^2} = \left(\frac{\pi f_0}{H}\right)\left[P_m - P_{\max}\sin\delta\right] \tag{2.6}$$

Writing equation 2.6 in a form suitable for analog implementation:

$$\delta \equiv V_0 = V_{IC2} + g\iint \left[I_m - I_e\left(V_0\right) \right] dtdt \tag{2.7}$$

The power angle δ is solved using general-purpose mathematical analog devices. Using the setup approach discussed in subsection 2.1, equation (2.7) can be rewritten in circuit form as shown in Figure 2.6. This is a case of a single generator connected to an infinite bus through a lossless transmission line.

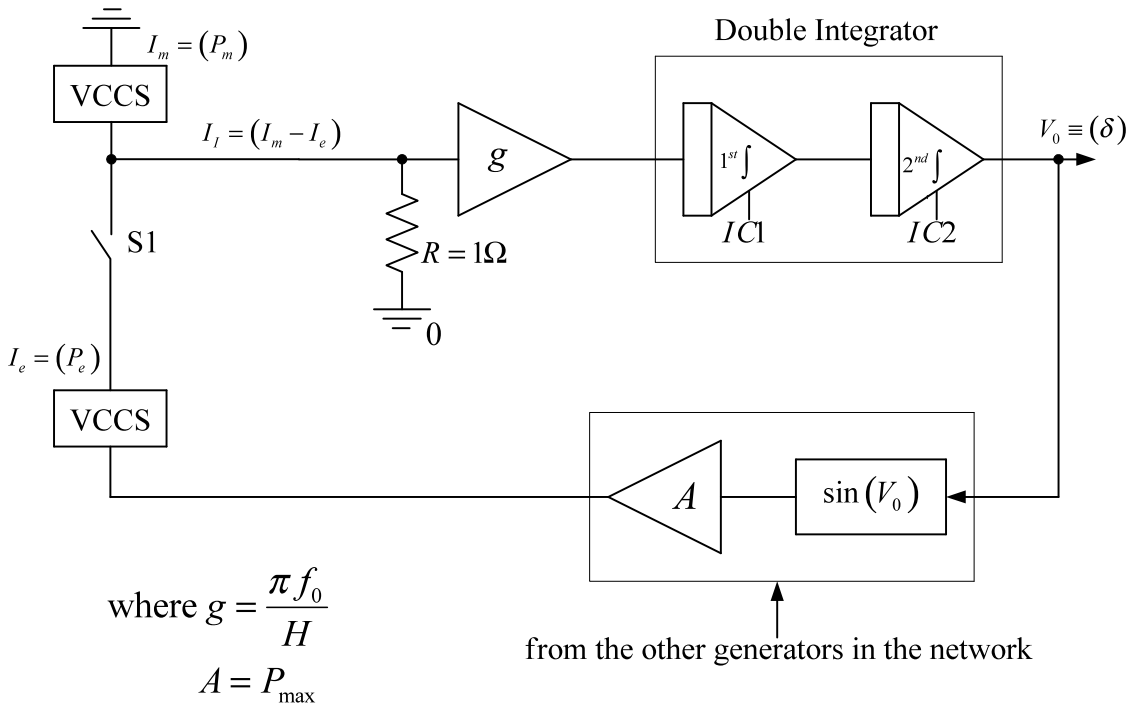

Figure 2.6: Analog Circuit Representation of Swing Equation

The output V_0 represents the electrical angle δ of the generator, as given by equation (2.7). In Figure 2.6 and equation (2.7), the currents I_m and I_e are used to represent mechanical and electrical power, respectively. The difference between these two currents is amplified by a constant $g\left(=\frac{\pi f_0}{H}\right)$ (generator and electrical system parameters) and fed into the double integrator. The sum of the output of the double integration process and the initial condition V_{IC2} is a voltage V_0, equivalent to the electrical angle δ in radians. The $I_e(V_0)$ in equation (2.7) represented as $A\sin(V_0)$ in Figure 2.6, describes the dependency of electrical power on the electrical angle.

The steady state solution of a generator dynamical equation is that value for which generator power angle δ is constant relative to the infinite bus. The complex voltage at a generator terminal is therefore its desired magnitude $|\mathrm{E}|$, and argument $\angle\delta$. Figure 2..7 below shows the block diagram of the generator module. The module contains the building blocks for solving the swing equation (dynamic) and also determining the complex voltage output for a single generator (static). A similar module will be used for each and every other generator in the network but with their own parameters. The power angle δ of the generator is split into real and imaginary components as illustrated by the coordinate transformation of Figure 2.7. This form is easier and more efficiently represented in analog circuits. Therefore, the real part of the generator terminal voltage is found by taking the cosine of δ and multiplying by $|E_g|$ as shown in Figure 2.7. Likewise, the imaginary part of the generator terminal voltage is found by

taking the sine of δ and multiplying by $|E_g|$. These component voltages are then fed into the real and imaginary parts of transmission network modules through generator terminals I^{I}, I^{II}, I^{III} and I^{IV} respectively. The sine (cosine) block outputs sine (cosine) value of its input signal. The current drawn from the generator's real and imaginary voltage sources are used to calculate the complex current drawn from the generator. The electrical power of the generator is computed according to equation (2.3) and methodology described in subsections 2.2 and 2.4.

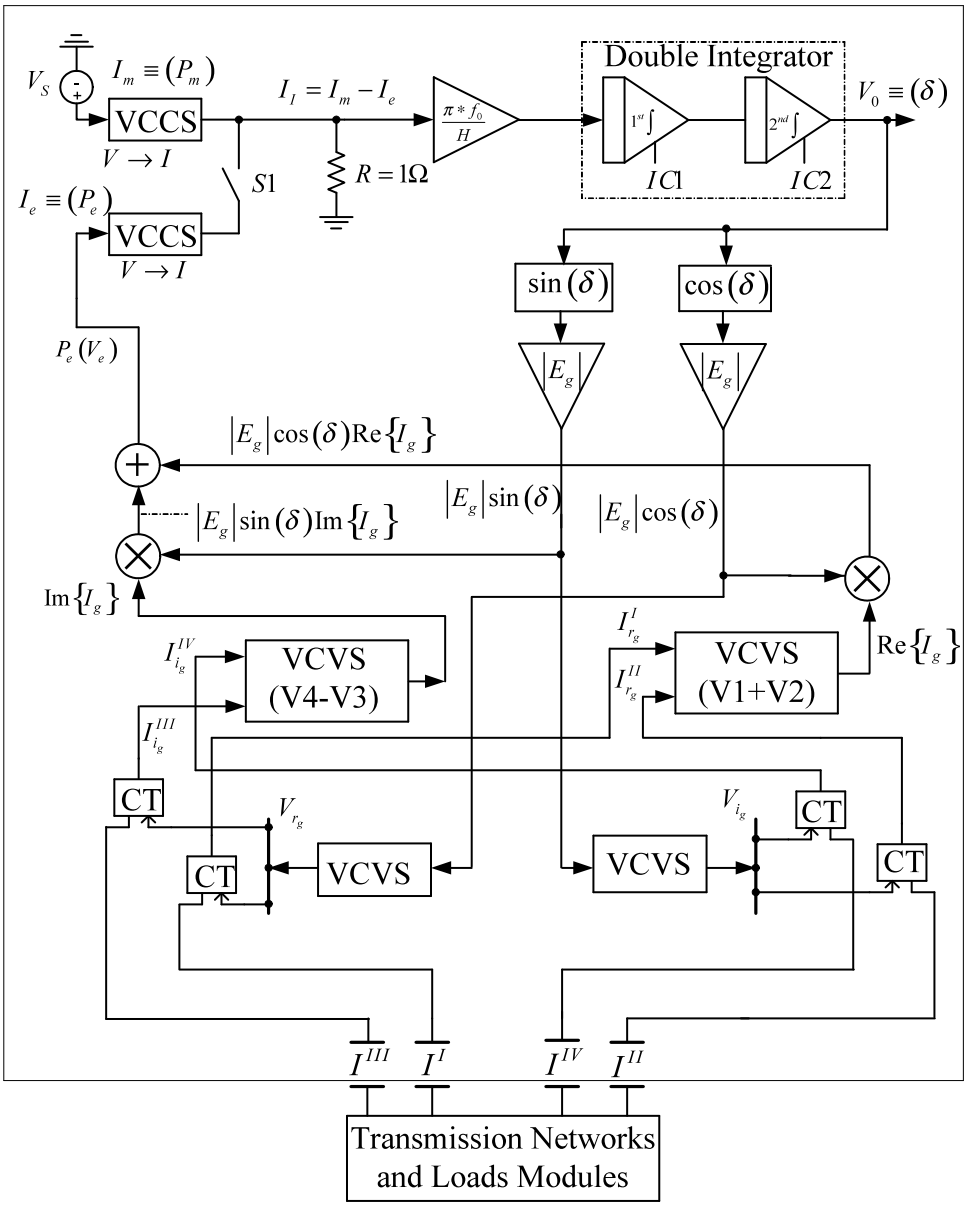

Figure 2.7: Block Diagram of Analog Emulator Generator Module

VCVS - Voltage Controlled Voltage Source; R - Resistor;
VCCS - Voltage Controlled Current Source; S1 - Switch;
$\mathrm{Re}\{I_g\}$ - Real part of generator current; V_S - Voltage Source;
$\mathrm{Im}\{I_g\}$ - Imaginary part of generator current; CT - Current Transformer;
I^I, I^{III} - Real Voltage Terminal; I^{II}, I^{IV} - Imaginary Voltage Terminal;
$P_m (\equiv I_m)$ - Mechanical Power (Equivalent Mechanical Current);
$P_e (\equiv I_e)$ - Electrical Power (Equivalent Electrical Current);
$I^I_{r_g}, I^{II}_{r_g} \left(I^{III}_{i_g}, I^{IV}_{i_g}\right)$ - real and imaginary part of component currents determined by network 1,2,3 and 4.

2.6.2 TRANSMISSION NETWORK MODULE

Several analog approaches for simulating or emulating transmission network are discussed in a technical paper by Fried, et al [28]. In this report, the approach of dc-resistive network is considered and discussed earlier. In order words, four separate dc-resistive networks will be required to emulate a power system transmission network. Figure 2.8 shows a general example of a three-bus power system and Figure 2.9 illustrates the principle of how four dc-resistive networks are used to emulate this sample three-bus power system.

Two dc-resistive networks (networks 1 & 4) to represent the real part of transmission line impedance and another two dc-resistive network to represent the imaginary part (networks 2 & 3). The transformation of the complex impedance of each branch to its resistive values is described by equation (2.1). For convenience, the equations are rewritten here as equation (3.21). The component voltage sources from generator

terminals I^{I}, I^{II}, I^{III} and I^{IV} are fed into the real and imaginary parts of transmission network modules as described in subsection 2.2. Then, the current I_{g_i} flowing out of generator i into the network is calculated. From the equation (2.2), it is clear that the real part of current flowing on any given branch of a real network is the sum of component currents flowing in emulated networks 1 and 2. Likewise, imaginary part of current flowing on any given branch of a real network is the difference of component currents flowing in emulated networks 4 and 3.

$$R_{\mathrm{Re}(Z_{ij})} = 1/\mathrm{Re}\{Y_{ij}\} = \frac{R_{ij}^2 + X_{L_{ij}}^2}{R_{ij}}$$
$$R_{\mathrm{Im}(Z_{ij})} = 1/\mathrm{Im}\{Y_{ij}\} = \frac{R_{ij}^2 + X_{L_{ij}}^2}{X_{Lij}} \qquad (2.8)$$

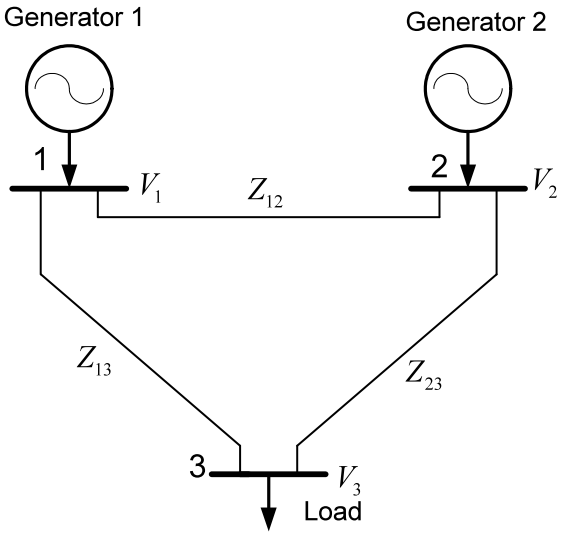

Figure 2.8: A Sample Three-Bus Power System

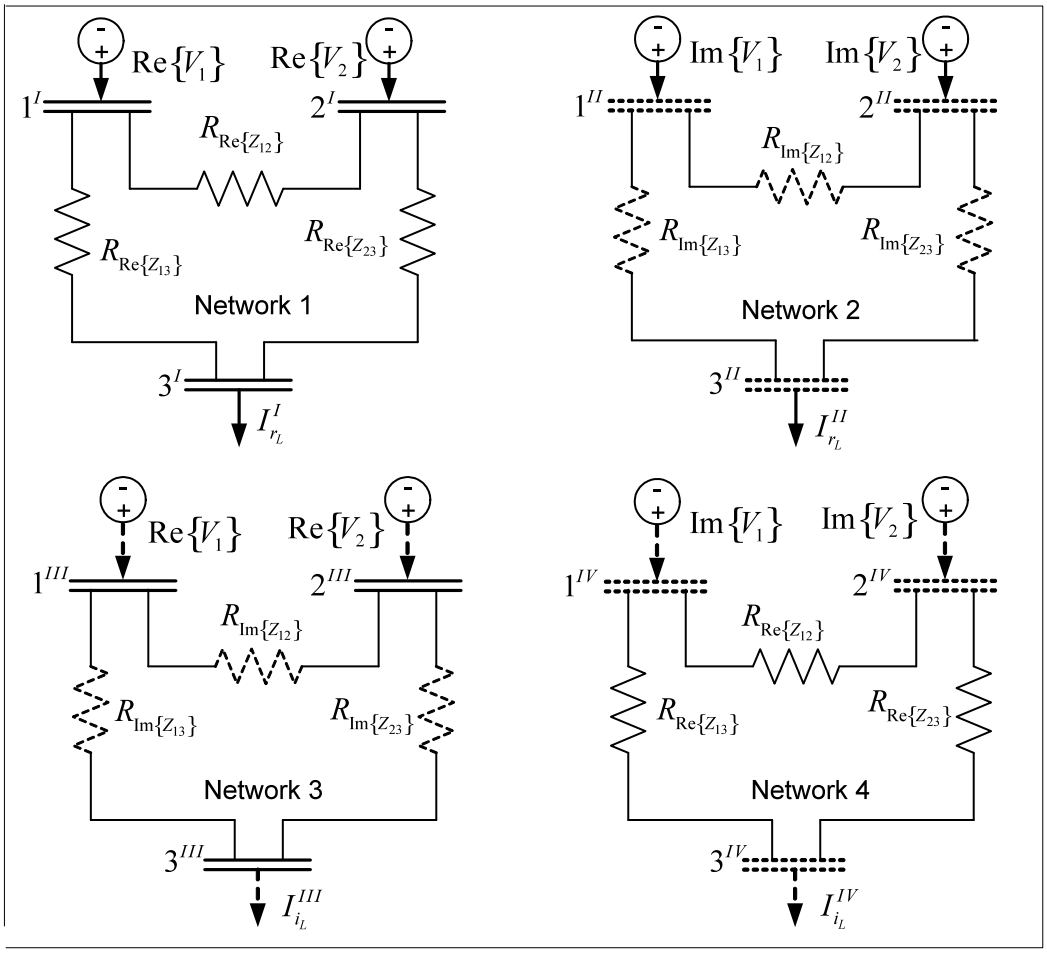

Figure 2.9: DC-Resistive Network Emulation Approach for Sample System

where:

$\mathrm{Re}\{V_i\}$ - Real part of voltage at generator bus *i*;

$\mathrm{Im}\{V_i\}$ - Imaginary part of voltage at generator bus *i*;

$\mathrm{Re}\{Z_{ij}\}$ - Real part of transmission line impedance between buses *i* & *j*;

$\mathrm{Im}\{Z_{ij}\}$ - Imaginary part of transmission line impedance between buses *i* & *j*;

$I_L^I, I_L^{II}, I_L^{III}, I_L^{IV}$ - Load current $(\equiv$ Load power$)$;

$1^*, 2^*, 3^*$ - Bus or node;

$(*)$ indicates corresponding network.

2.6.3 LOAD MODULE

A differential form of constant PQ-Load model [45,46] is used to build the emulator load module. Separate modules will be required for each power system load representation. If the voltage drop across the load and the current into the load are expressed as $V = |\mathrm{V}| \angle \theta_V$ and $I = |\mathrm{I}| \angle \theta_I$, respectively, the product of voltage times the conjugate of current in polar form will give the complex power being absorbed by the load. That is,

$$S = VI^* = |\mathrm{V}||\mathrm{I}| \angle \theta_V - \theta_I \tag{2.9}$$

or in rectangular form as

$$S = VI^* = |\mathrm{V}||\mathrm{I}| \cos(\theta_V - \theta_I) + j|\mathrm{V}||\mathrm{I}| \sin(\theta_V - \theta_I) \tag{2.10}$$

If $\theta_V - \theta_I = \theta$ is the phase angle between voltage and current, then

$$\begin{aligned} &S = P + jQ \\ &\text{where } P = |\mathrm{V}||\mathrm{I}| \cos\theta \text{ and } Q = |\mathrm{V}||\mathrm{I}| \sin\theta \end{aligned} \tag{2.11}$$

Rewriting equation (2.10) using Figure 2.7 as

$$\begin{aligned} S = VI^* &= (V_r + jV_i)(I_r - jI_i) \\ &= V_r I_r + V_i I_i + j(V_i I_r - V_r I_i) \\ \text{where } V_r &= |\mathrm{V}| \cos\theta \text{ and } V_i = |\mathrm{V}| \sin\theta \\ I_r &= |\mathrm{I}| \cos\theta \text{ and } I_i = |\mathrm{I}| \sin\theta \end{aligned} \tag{2.12}$$

As mentioned earlier, the loads are represented by frequency and voltage dependent models, that is,

$$\left.\begin{aligned} P_L + K_{p\theta}\dot{\theta} &= P_e \\ Q_L + K_{qv}\dot{V} &= Q_e \end{aligned}\right\} \tag{2.13}$$

The first order integration of equation (2.13) yields

$$\left.\begin{aligned} \theta &= \frac{1}{K_{p\theta}}\int\left(-P_L + P_e\right)dt \\ |\mathrm{V}| &= \frac{1}{K_{qv}}\int\left(-Q_L + Q_e\right)dt \end{aligned}\right\} \tag{2.14}$$

That is, the load bus phase angle is very sensitive to the difference in the real load and real electrical power as the load bus voltage magnitude is very sensitive to the difference in the reactive load and reactive electrical power. Using equations (2.12) and (2.14), ABMs are used to build a constant PQ load module as described in Figure 2.10.

In summary, generators and constant PQ loads are modeled using general-purpose analog components. That is, the mathematical equations that describe the state of these components of real power system are represented using electrical circuit equivalents (ABMs). The transmission networks are represented as a scaled-down model. Interconnecting these three components will give a complete power system.

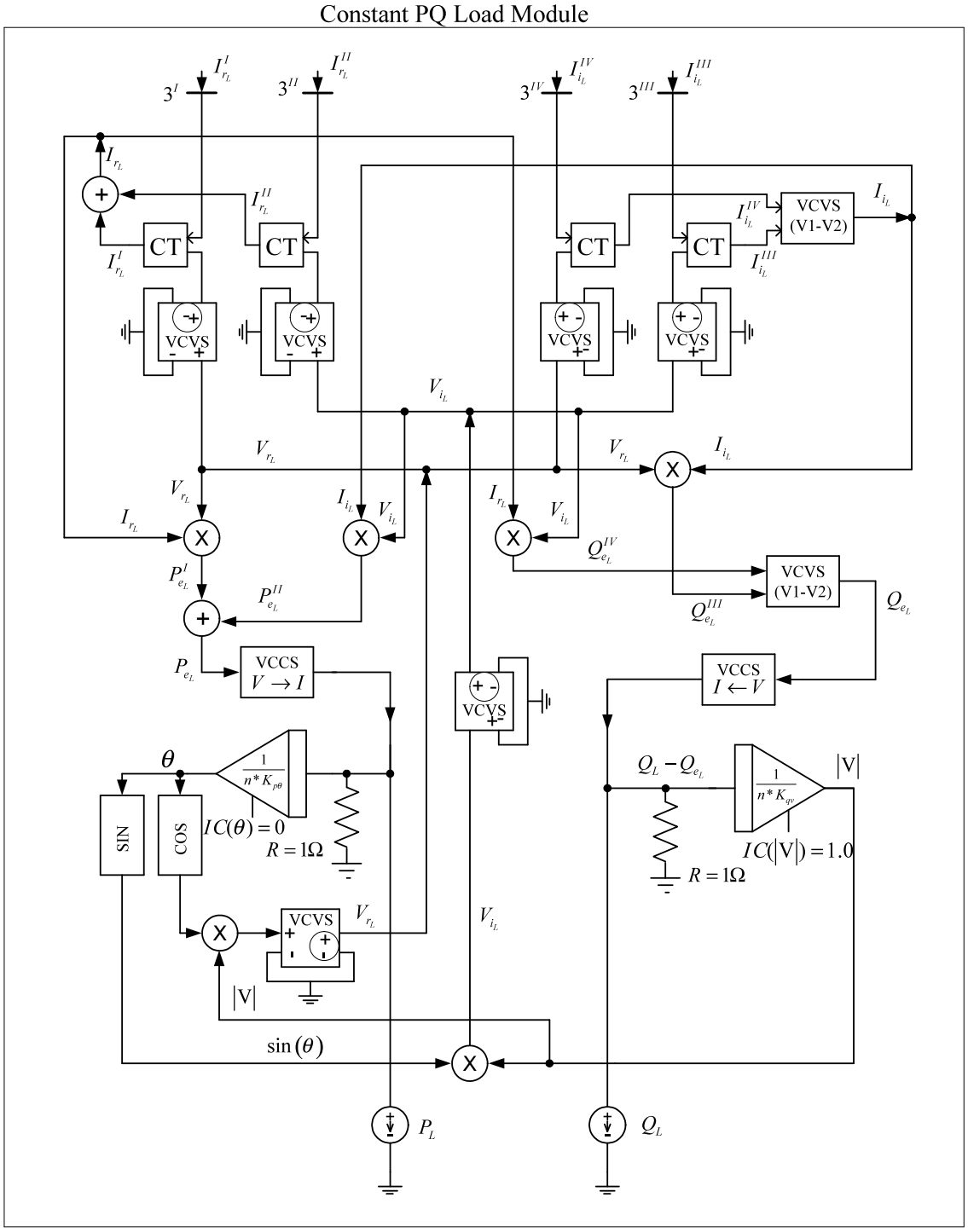

Figure 2.10: Constant PQ Load Modules (Differential Form)

where

CT - Current Transformer

VCVS - Voltage Controlled Voltage Source

VCCS - Voltage Controlled Current Source

$I_{r_L}^{I}, I_{r_L}^{II}, I_{i_L}^{III}$ and $I_{i_L}^{IV}$ - are load component currents

$P_{e_L} = P_{e_L}^{I} + P_{e_L}^{II}$ - load electrical active power with its components

$Q_{e_L} = Q_{e_L}^{IV} - Q_{e_L}^{III}$ - load electrical reactive power with its components

P_L and Q_L - real and reactive given load values

IC - initial conditions

For feasible load bus voltage computation, it is very crucial that the integrators that compute the load bus voltage magnitude and angle be initialized to 1 and 0, respectively. Also, values of the exponential recovery rate of angle and voltage magnitude must be set.

3. VALIDATION OF ANALOG EMULATOR MODULE

3.1 OVERVIEW

The analog emulator component modules that were developed in Chapter 3 were tested on sample 3, 6 and 14-bus power systems, as described in Appendix A. Tests were conducted on each of the cases by running PSpice simulations [44] of the analog emulator built on Analog Behavioral Models (ABMs) and analog devices in PSpice design environment. PSpice circuits for each case are described in Appendix B. The same sample power systems were run on industrial grade numerical simulation software; PowerWorld v.9.1 [42] and Power System Simulator for Engineers (PSS/E) v.28.1 [43], for benchmarking (see Appendix C). For the validation, the following parameters were measured or calculated and compared with the benchmarks:

i. δ_{j1} - voltage angle difference between generator buses j and 1, (j=2, 3, …);

ii. Load bus complex voltage;

iii. Complex current flowing in each branch.

Simulation results obtained from the proposed analog emulator and those of the benchmarks are presented in section 3.4 and Appendix C.

Figure 3.1 below is a sample 3-bus power system with parameters given in Table 4.1. Details of analog emulator system setup for the sample are discussed in section 3.2. Other test cases are described in Appendix A.

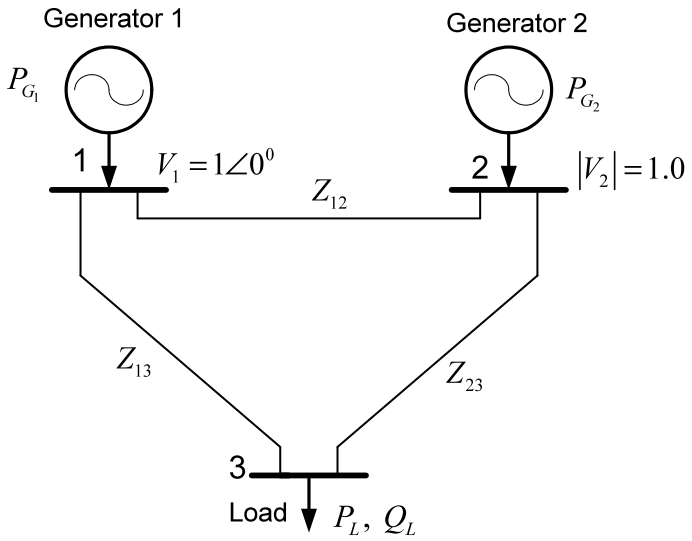

Figure 3.1: Sample 3-Bus Systems

Table 3.1: System Parameters for a Sample 3-Bus System

Bus Data (pu)					Line Data for Lossless System (pu)		Line Data for Lossy System (pu)	
Bus #	P	Q	H	D				
Bus 1	-	-	-	-	X_{12}	0.02	R_{12}	0.01
							X_{12}	0.01
Bus 2	2.0	-	4s	-	X_{13}	0.03	R_{13}	0.02
							X_{13}	0.01
Bus 3	3.0	0.5	-	-	X_{23}	0.06	R_{23}	0.012
							X_{23}	0.025

3.2 ANALOG EMULATOR SYSTEM SETUP

An analog emulator was built based on the approach and methodology as described in Chapter 3. A scaled-down equivalent of a real power system short transmission line model is used to build a transmission network module using the dc-network approach, while general purpose mathematical analogs are the basis for generator and load modules. Steps for the emulator setups are discussed in the following subsections.

3.2.1 MATHEMATICAL EQUATIONS TRANSFORMATION

The mathematical equations describing the states and behaviors of power system components are transformed to its analog circuit's equivalent using general-purpose mathematical analogs as described in subsection 2.2. In this report, these steps apply to generators and loads. The development of generator module using ABMs is discussed in subsection 2.6.1. Constant PQ-load (differential form) module is developed in subsection 2.6.3. For convenience purposes, these equations are rewritten.

For generators:

$$\frac{H}{\pi f_0}\frac{d^2\delta}{dt^2} = P_m - P_e \tag{3.1}$$

For loads:

$$\left.\begin{aligned} P_L + K_{p\theta}\frac{d\theta}{dt} &= P_e \\ Q_L + K_{qv}\frac{d|\mathrm{V}|}{dt} &= Q_e \end{aligned}\right\} \tag{3.2}$$

3.2.2 APPLICATION OF SCALE FACTORS

The computation speed of an unscaled analog emulator for any given size of a system is approximately equal to the physical system real-time speed. In this report, time-scale factor of $n = 0.001$ is used. That is, emulator computation time is sped up 1000 times faster than real-time speed of the physical system, or

$$n = \frac{\tau}{t} = \frac{1}{1000} = 0.001 \tag{3.3}$$

The magnitude-scale factor used can be referred to as per-unit scaling. Two independent base values chosen for power system test samples are base line-to-line voltage and three-phase base complex power. That is:

$$\left.\begin{aligned} S_b^{3\phi} &= 100MVA \\ V_b^{LL} &= 69kV \end{aligned}\right\} \tag{3.4}$$

The following relations which must obey circuit laws are also used:

$$P_b = Q_b = S_b \tag{3.5}$$

$$Z_b = R_b = X_b \tag{3.6}$$

$$I_b = \frac{S_b^{3\phi}}{\sqrt{3}V_b^{LL}} \tag{3.7}$$

$$Z_b = \frac{V_b^{\phi}}{I_b} = \frac{(V_b^{LL})^2}{S_b^{3\phi}} \tag{3.8}$$

The value of the magnitude scaling constant $C_x = 1$, for all magnitude transformation since ABMs input/output values fall within acceptable ranges. In a case where there is need for further reduction in magnitude of a parameter, C_x of affected quantity takes a value less than 1. Therefore, actual values of power system parameters of Figure 3.1 and Table 3.1 are:

$$P_3 = P_{3_{pu}} * S_b = 3.0 * 100 = 300MW$$
$$Q_3 = Q_{3_{pu}} * S_b = 0.5 * 100 = 50M \text{ var}$$
$$|V|_2 = |V|_{2_{pu}} * V_b = 1.0 * 69kV = 69kV$$
$$X_{23} = X_{23_{pu}} * Z_b = 0.06 * 47.61 = 2.8566\ \Omega$$

where

$$I_b = \frac{S_b^{3\phi}}{\sqrt{3}V_b^{LL}} = \frac{100 * 10^6}{\sqrt{3} * 69 * 10^3} = 836.74 \text{ A} \tag{3.9}$$

$$Z_b = \frac{V_b^{\phi}}{I_b} = \frac{(V_b^{LL})^2}{S_b^{3\phi}} = \frac{(69 * 10^3)^2}{100 * 10^6} = 47.61\ \Omega \tag{3.10}$$

Applying time and magnitude scale factors to all independent variables of generator and load equations (3.1) and (3.2), respectively:

$$\delta = \frac{1}{(0.001)^2}\frac{\pi f_0}{H}\iint (P_m - P_e)dtdt \tag{3.11}$$

$$\left.\begin{aligned} \theta &= \frac{1}{0.001}\frac{1}{K_{p\theta}}\int (-P_L + P_e)dt \\ |\mathrm{V}| &= \frac{1}{0.001}\frac{1}{K_{qv}}\int (-Q_L + Q_e)dt \end{aligned}\right\} \tag{3.12}$$

Sample plots of the generator power angle δ which is the solution of swing equation (3.11) over time is depicted in Figures 3.2 and 3.3 for case where time-scale factor $n=1$ and $n=0.001$ respectively. The observation window of simulation time is extended over 100 seconds for transients to fully settle down. From the plots, it can be seen that the steady state value of δ is the same in both cases, but the time to reach this value is different. In Figure 3.2, with $n=1$, δ reaches steady state after 10s while in Figure 3.3 with $n=0.001$, the steady state value is attained within 0.01s which is 1000 times faster than the former. It should also be mentioned that magnitude scaling (not applied here) has an additional effect not only on the size of power system that can be mapped on a given size of an analog emulator but also on its speed of computation (for example, capacitor time constant).

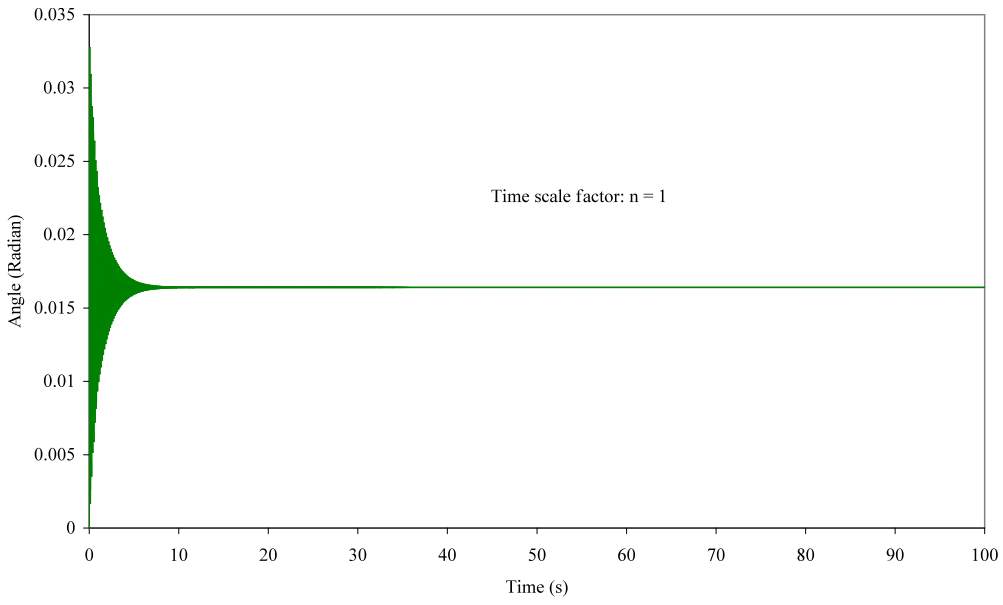

Figure 3.2: Time Scaling Effect on Analog Emulator Computation

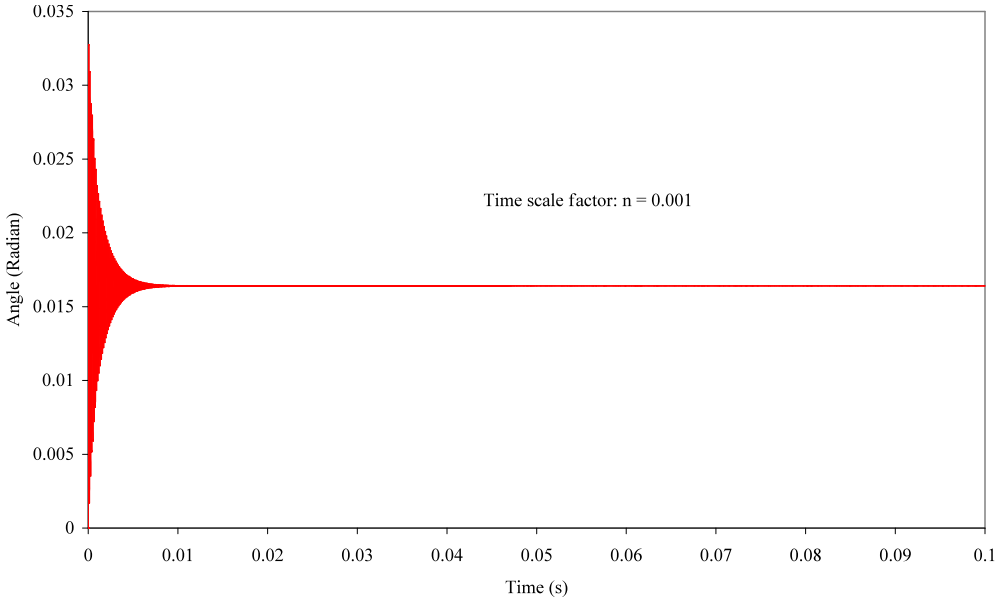

Figure 3.3: Time Scaling Effect on Analog Emulator Computation

3.2.3 SETTING OF INITIAL CONDITIONS AND OTHER CONSTANTS

It is important to initialize parameter values and initial conditions of the integrators. In this emulator, parameters that need to be set are terminal voltage magnitudes of generators, generators input mechanical powers from prime movers $P_m(I_m)$, inertia constants H, and loads values $P_L, Q_L(I_{P_L}, I_{Q_L})$. In addition, the exponential recovery rate of angle and voltage magnitude $K_{p\theta}$ and K_{qv}, respectively, of the constant-PQ load model differential form must be set.

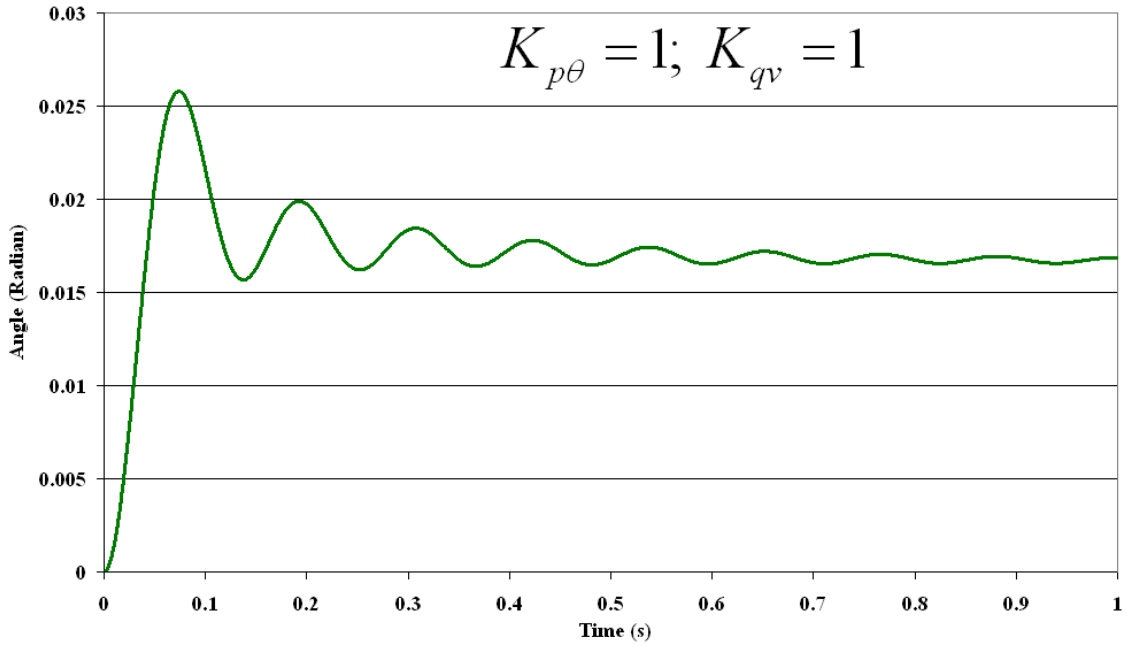

Figure 3.4: Effect of $K_{p\theta}$ and K_{qv} on Computation of Generator Relative Angles

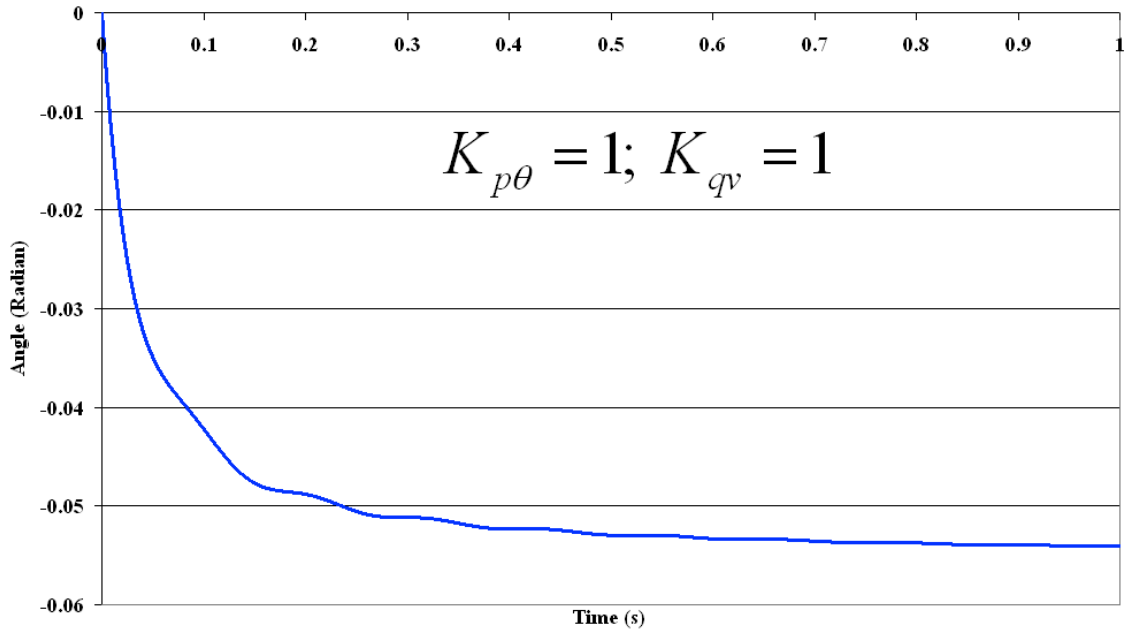

Figure 3.5: Effect of $K_{p\theta}$ and K_{qv} on Computation of Load Bus Phase Angle

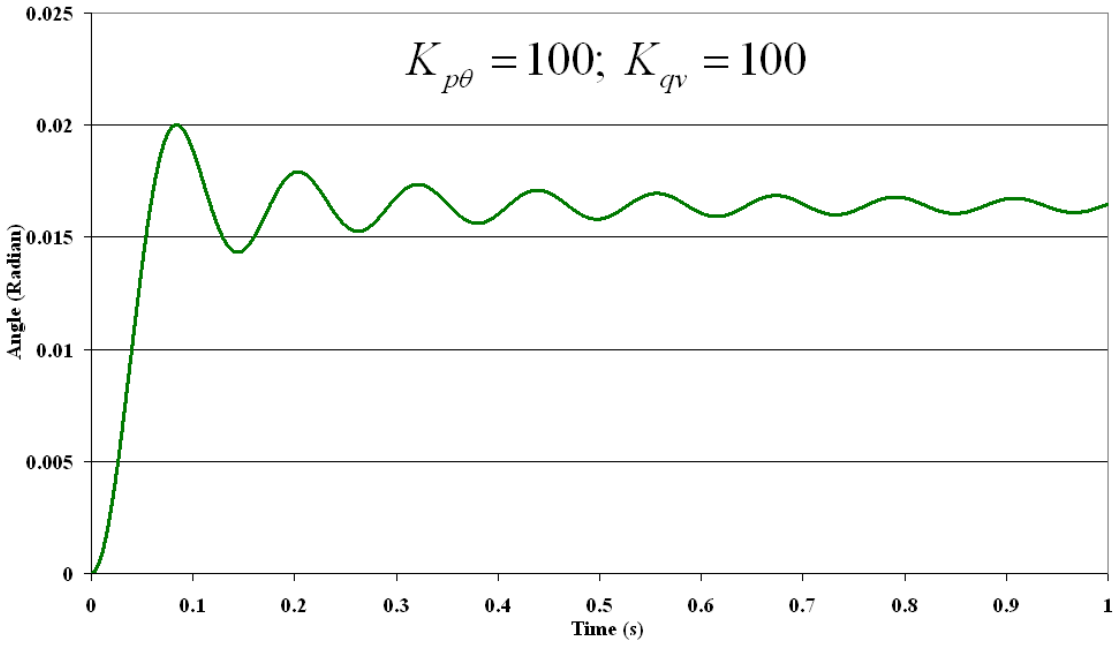

Figure 3.6: Effect of $K_{p\theta}$ and K_{qv} on Computation of Generator Relative Angles

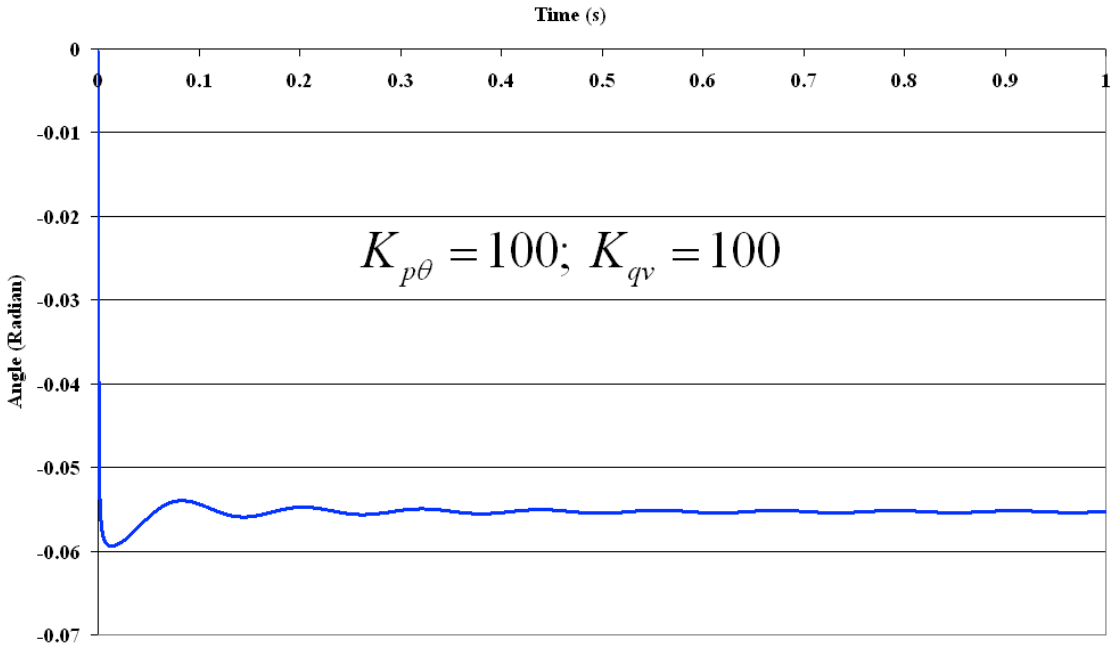

Figure 3.7: Effect of $K_{p\theta}$ and K_{qv} on Computation of Load Bus Phase Angle

Figures 3.4 through 3.7 show the effect of $K_{p\theta}$ and K_{qv} on the computation of generators relative angles and load-bus phase angles. Case of $K_{p\theta} = K_{qv} = 1$ is depicted in Figures 3.4 and 3.5, and case of $K_{p\theta} = K_{qv} = 100$ in Figures 3.6 and 3.7. It can be observed that the computation of load-bus phase angle took a longer time to arrive at a steady state value in the case of $K_{p\theta} = K_{qv} = 1$ when compared to $K_{p\theta} = K_{qv} = 100$. Also, the first swing of generator's relative angle is higher in the case of $K_{p\theta} = K_{qv} = 1$ than with $K_{p\theta} = K_{qv} = 100$, but settled to steady state quicker than the latter.

Ideally, it is desirable for the load-bus phase angle to solve faster and reach steady-state quicker than the generator bus (this emulates real life behavior). The PSpice design and simulation environment used in this report did not allow detailed investigation and characterization of the effect of the coefficients of the exponential recovery rate of an angle $K_{p\theta}$ and exponential recovery rate of voltage magnitude K_{qv}, due to some convergence problems.

3.2.4 RATIONALIZATION OF COMPLEX IMPEDANCE VALUES OF THE TRANSMISSION LINES

Rationalization of complex impedance values of transmission line is necessary because of the dc-network emulation approach used. Using equation (2.1), branch impedance complex values are transformed into their rationalized resistance values as shown in Tables 4.2 and 4.3 below. For the lossless network where real part of complex impedance R=0, its transformed value $R_{\mathrm{Re}\{Z_{ij}\}} = \infty$, but represented as $R_{\mathrm{Re}\{Z_{ij}\}} = 1G\Omega$ in the circuit implementation. The idea of making this value very large is to create open circuit or minimize current flowing in the equivalent dc-networks I and IV. Alternatively, networks I and IV may be removed. Removing networks I and IV for a lossless system simulation may be cumbersome, as the generator and load modules will also require modifications.

Table 3.2: Transmission Network Impedance of a Sample 3-Bus Power System

	R_{12}	X_{12}	R_{13}	X_{13}	R_{23}	X_{23}
Lossless Network (pu)	0	0.02	0	0.03	0	0.06
Lossy Network (pu)	0.01	0.01	0.02	0.01	0.012	0.025

Table 3.3: DC-Network Equivalent Impedance of Table 4.2

	$R_{\mathrm{Re}\{Z_{12}\}}$	$R_{\mathrm{Im}\{Z_{12}\}}$	$R_{\mathrm{Re}\{Z_{13}\}}$	$R_{\mathrm{Im}\{Z_{13}\}}$	$R_{\mathrm{Re}\{Z_{23}\}}$	$R_{\mathrm{Im}\{Z_{23}\}}$
Lossless Network (pu)	1×10^{6}	0.02	1×10^{6}	0.03	1×10^{6}	0.06
Lossy Network (pu)	0.02	0.02	0.025	0.05	0.0641	0.03076

It should be mentioned that the negative in $R_{\mathrm{Im}\{Z_{ij}\}}$ component of equation (2.1) is taken care of during complex current computation implementation, as shown in Figure 2.3.

3.2.5 VARIABLES AND PARAMETERS REPRESENTATION IN ANALOG EMULATION IMPLEMENTATION

For convenience and efficient analog emulation implementation, certain power system variables and parameters are represented by other circuit variables. Also, ABMs only accept voltage(s) as input(s) and output voltage except in the case of Voltage Controlled Current Source (VCCS) where the output is current. Therefore, there are cases in the modules where current is represented as voltage or power as current. However, since the conversion ratio used between current-voltage or power-current is 1:1, obtained values remain representative in quantity. Figure 3.8 below summarizes variable representations used in this report.

$$\left.\begin{matrix} P \\ Q \end{matrix}\right\} \rightarrow I \text{ (1 pu : 1 A)}$$
$$\delta \rightarrow V \text{ (1 radian : 1 volt)}$$
$$I \rightarrow V \text{ (1 A : 1 volt)}$$

Figure 3.8: Variable Representation in Analog Emulator

3.3 SIMULATION RESULTS

The analog emulator modules have the capability of solving steady state load flow. They can as well be used for solving transient stability problem for cases of an electrical fault on the generator terminal. Generators relative power angle, branch currents in the network and buses voltages can be measured in real and continuous time. For the slack generator, ordinary constant voltage source is used, to serve as reference and maintain desired voltage magnitude and angle. All other angles are measured relative to the slack generator power angle. Modules of generator, transmission networks, loads and test systems built on ABMs and analog devices are depicted in Appendix B.

Measurements and readings from PSpice runs for load flow of sample 3-bus power system are presented next. Figure 3.9 shows steady state solution of relative power angle between generator 2 and slack generator for a case of lossless transmission system. Figure 3.10 and 3.11 show load bus voltage magnitude in per unit and relative angle in radians, respectively. These measurements are taken out of the module described in Figure B1. Summary results for all test system and their comparisons with the industrial grade numerical simulators are presented in section 3.4. Detail simulation results which include PSS/E interface printouts, power-flow diagrams of PowerWorld and graphical plot of measurements at various points of interest in the analog emulator circuits are given in Appendix C.

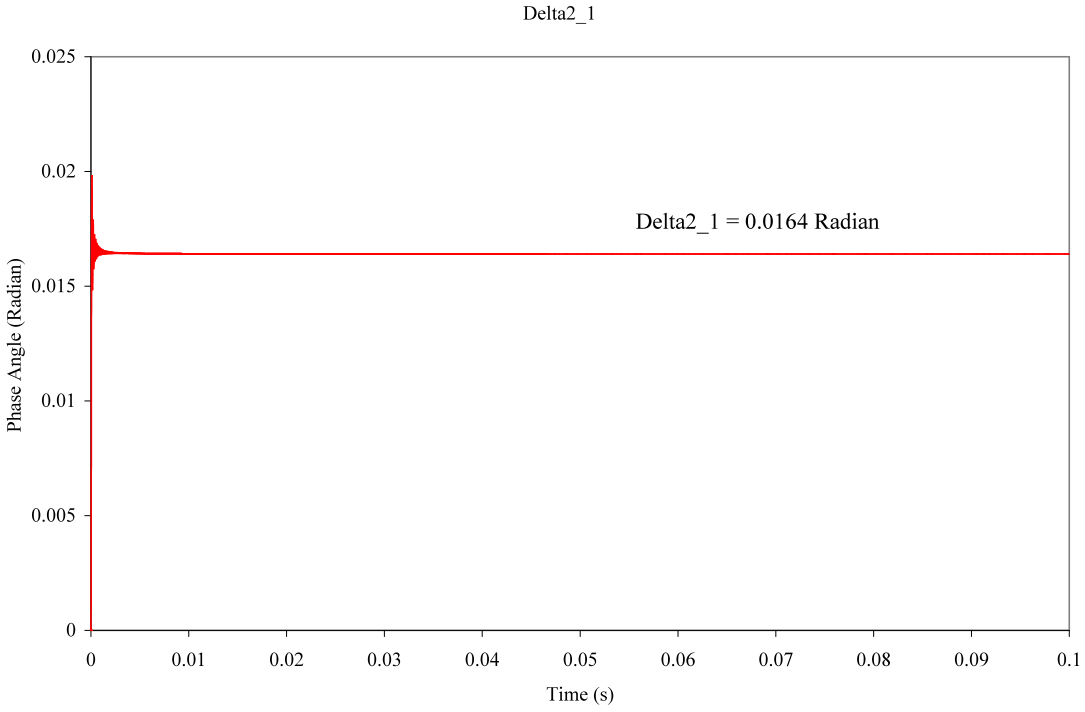

Figure 3.9: Steady State Relative Power Angle between Generators 2 and 1

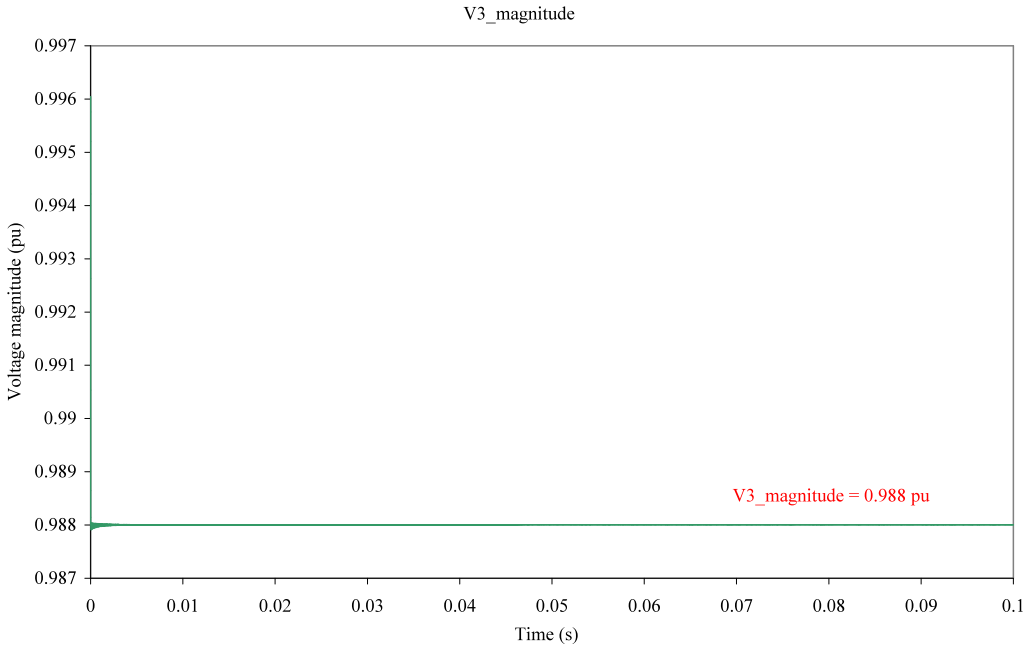

Figure 3.10: Load Bus (V3) Voltage Magnitude

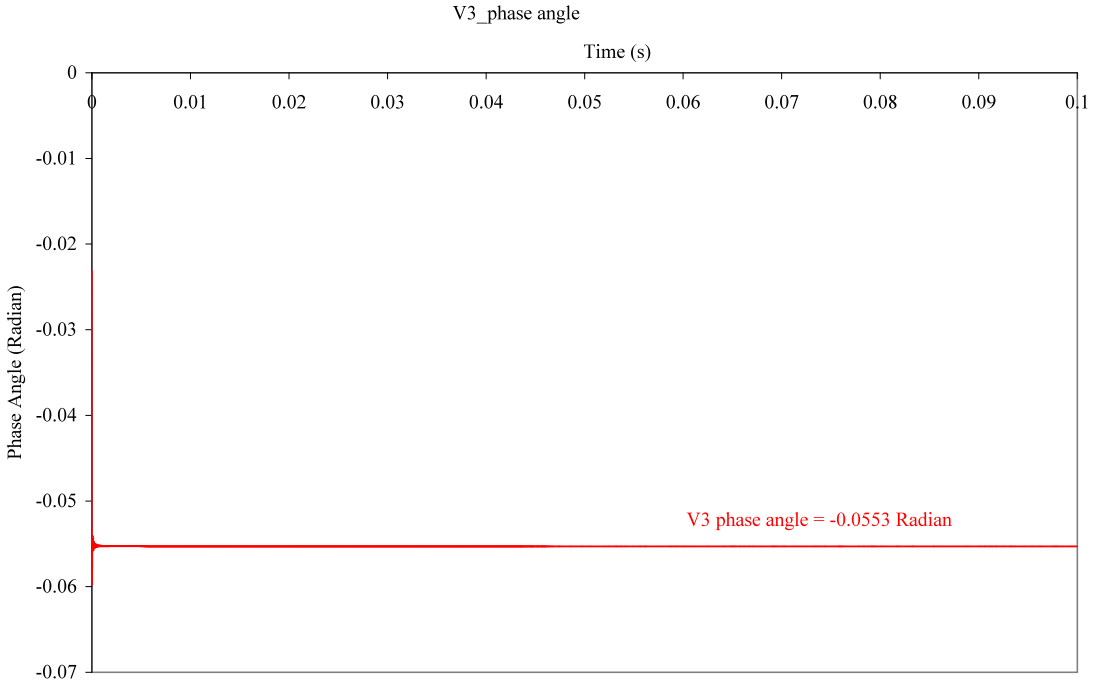

Figure 3.11: Load Bus (V3) Phase Angle

3.4 RESULTS COMPARISONS AND COMMENTS

Summary results from the PowerWorld and PSS/E which serve as benchmark and the proposed analog emulator are described in Table 4.4 through 4.7 for different test system. From the tables it could be concluded that results of steady state load flow values from analog emulator compare relatively well with those of the benchmarks (PowerWorld and PSS/E).

Table 3.4: Summary Results for a 3-Bus Power System (Lossless Case)

	PowerWorld	PSS/E	Analog Emulator
Relative Power Angle (δ_{21}) in degree	0.94^0	0.9^0	0.94^0
Load Bus (V3) Voltage (V_{pu})	$0.988\angle -3.17^0$	$0.988\angle -3.2^0$	$0.988\angle -3.17^0$
Current in Branch 2_1 $(I,\ \mathrm{A})$	686.37	686	$686.37\angle 0.47^0$
Current in Branch 1_3 $(I,\ \mathrm{A})$	1568.99	1569	$1569\angle -13.91^0$
Current in Branch 2_3 $(I,\ \mathrm{A})$	1007.73	1008	$1007.77\angle -10.70^0$

Table 3.5: Summary Results for a 3-Bus Power System (Lossy Case)

	PowerWorld	PSS/E	Analog Emulator
Relative Power Angle (δ_{21}) in degree	0.65^0	0.6^0	0.65^0
Load Bus (V3) Voltage (V_{pu})	$0.968\angle -1.03^0$	$0.968\angle -1^0$	$0.968\angle -1.03^0$
Current in Branch 2_1 $(I,\ \mathrm{A})$	668.52	669	$669.22\angle 45.30^0$
Current in Branch 1_3 $(I,\ \mathrm{A})$	1382.78	1383	$1383.2\angle 1.36^0$
Current in Branch 2_3 $(I,\ \mathrm{A})$	1308.47	1308	$1308.4\angle -23.1^0$

Table 3.6: Summary Results for a 6-Bus Power System (Lossy Case)

	PowerWorld	PSS/E	Analog Emulator
Relative Power Angle (δ_{21}) in degree	-2.10^0	-2.1^0	-2.10^0
Relative Power Angle (δ_{31}) in degree	-2.71^0	-2.7^0	-2.71^0
Load Bus (V4) Voltage (V_{pu})	$0.974\angle -7.35^0$	$0.974\angle -7.3^0$	$0.974\angle -7.35^0$
Load Bus (V5) Voltage (V_{pu})	$0.988\angle -4.69^0$	$0.988\angle -4.7^0$	$0.988\angle -4.69^0$
Load Bus (V6) Voltage (V_{pu})	$0.983\angle -6.36^0$	$0.983\angle -6.4^0$	$0.9829\angle -6.36^0$
Current in Branch 1_2 $(I,\ \mathrm{A})$	344.86	345	$344.86\angle -29.76^0$
Current in Branch 1_5 $(I,\ \mathrm{A})$	758.72	759	$758.72\angle -20.98^0$
Current in Branch 2_5 $(I,\ \mathrm{A})$	388.84	389	$388.84\angle -15.95^0$
Current in Branch 2_6 $(I,\ \mathrm{A})$	515.047	515	$515.04\angle -11.7^0$
Current in Branch 3_6 $(I,\ \mathrm{A})$	376.53	377	$376.54\angle -32.34^0$

Table 3.7: Summary Results for a 14-Bus Power System (Lossless Case)

	PowerWorld	PSS/E	Analog Emulator
Relative Power Angle (δ_{21}) in degree	-1.08^0	-1.1^0	-1.08^0
Relative Power Angle (δ_{31}) in degree	-0.75^0	-0.8^0	-0.75^0
Relative Power Angle (δ_{61}) in degree	-8.09^0	-8.1^0	-8.09^0
Relative Power Angle (δ_{81}) in degree	-7.30^0	-7.3^0	-7.30^0
Load Bus (V4) Voltage (V_{pu})	$0.989\angle -5.51^0$	$0.989\angle -5.5^0$	$0.989\angle -5.51^0$
Load Bus (V5) Voltage (V_{pu})	$0.991\angle -4.75^0$	$0.991\angle -4.8^0$	$0.991\angle -4.75^0$
Load Bus (V7) Voltage (V_{pu})	$0.984\angle -9.22^0$	$0.984\angle -9.2^0$	$0.984\angle -9.22^0$
Load Bus (V9) Voltage (V_{pu})	$0.979\angle -11.15^0$	$0.979\angle -11.2^0$	$0.979\angle -11.15^0$
Load Bus (V10) Voltage (V_{pu})	$0.980\angle -11.68^0$	$0.980\angle -11.7$	$0.980\angle -11.68^0$
Load Bus (V11) Voltage (V_{pu})	$0.987\angle -10.7^0$	$0.987\angle -10.7^0$	$0.987\angle -10.70^0$
Load Bus (V12) Voltage (V_{pu})	$0.982\angle -12.42^0$	$0.982\angle -12.4$	$0.982\angle -12.88^0$
Load Bus (V13) Voltage (V_{pu})	$0.980\angle -12.88^0$	$0.980\angle -12.9^0$	$0.980\angle -12.88^0$
Load Bus (V14) Voltage (V_{pu})	$0.979\angle -11.2^0$	$0.979\angle -11.2^0$	$0.979\angle -11.20^0$
Current in Branch 1_5 (I, A)	311.63	312	$311.63\angle 8.52^0$
Current in Branch 2_5 (I, A)	309.85	310	$309.85\angle 10.86^0$
Current in Branch 5_4 (I, A)	262.50	263	$262.50\angle 12.84^0$
Current in Branch 4_9 (I, A)	151.21	151	$151.21\angle 14.42^0$

It must be mentioned that there will be a convergence problem in the PSpice simulation:

i. If the time scale factor in the generator and load are not properly selected. This problem is likely attributed to PSpice software as it cannot respond to step function;

ii. If the constant multiplying the integrator input as in equations (3.11) and (3.12) is higher than order of magnitude 10^6 and 10^5 for the generator and load, respectively.

The conclusions of this research work, its contributions and recommendations for future research are discussed in the next section.

4. CONCLUSIONS AND FUTURE WORK

4.1 CONCLUSIONS

This report explored the feasibility of implementation of analog emulation of large-scale power systems using ABMs and analog devices in the PSpice design environment. The end goal is to develop a fast, programmable, and reconfigurable power system emulator using analog/mixed signal VLSI chips. Its computation time will be real-time and faster than real time and independent of the size of the power system. This report however, is the first step towards attaining this goal. ABMs and analog devices are used to develop modules of generators, transmission network and load using classical generator model, dc-resistive network equivalent of short transmission line model and constant-PQ load differential form model, respectively. The approach provided a large picture of the end goal, insight of design methodology of power system core computation and modules verification prior to full structural design and implementation.

The approach to the analog implementation of the power system emulator is based on an equivalent dc-network model that preserves the original power system network topology. In this technique, the complex variables and network parameters were transformed and expressed in rectangular coordinates. In rectangular coordinates the mathematical equations that describe the behavior of generator and load under various conditions are set up and evaluated using general purpose mathematical analog

(integration, summing, and multiplication operations). Transmission networks are represented as scaled-down model using resistors.

For the purpose of validating this approach, tests were conducted by running PSpice simulations of these analog emulation circuits for a sample 3, 6, and 14 bus power systems. The results of power flow simulations were compared with results obtained by running the same samples on other industrial grade numerical simulation software; PowerWorld v.9.1 and Power System Simulator for Engineers (PSS/E) v.28.1. The results matched favorably and confirmed the accuracy and validity of the approach. It should be mentioned however, that the speed of computation of analog emulator is real-time and can be faster than real time, depending on the time-scale factor used in the setup and independent of the size of the network or network topology.

Analog Behavioral Models and PSpice simulation software has been a very useful tool. Among other advantages mentioned previously is that: it gives opportunity to test-drive ideas, it aids in exploring the effects of modifications, etc. However, it should be mentioned that PSpice is not a prototype substitute; it gives hint but does not provide real final answer. As PSpice simulation helps, it may also mislead; PSpice simulations in this report are free of noise, crosstalk, interference, etc. In the actual implementation, there may be problems like noise, stray conductive paths and bias currents on the breadboard circuits to deal with. Also, component models of PSpice simulation used in this report are considered ideal. In real life, there may be effects like component variations, temperature, etc on the accuracy of the model.

4.2 SUMMARY OF RESEARCH CONTRIBUTIONS

Some key research contributions are highlighted below:

- Developed a module of constant PQ load differential form for analog emulator;
- In-house validation of analog emulator module using scaled-analog devices and ABMs representations of mathematical equations that describe the behaviors of power systems under various conditions;
- Proposed a methodology that leads to computationally feasible analog devices operation for accurate power system emulation.

4.3 FUTURE WORK

This report is just the first step towards a goal of developing a fast, programmable, and reconfigurable power system emulator using analog/mixed signal VLSI chip. The ABMs used are not real physical objects, circuit elements or blocks but ideal models based on sets of mathematical equations or transfer functions that describe the behavior of a circuit element or an analog building block. Real analog devices must be used to build mathematical functions such as integrators, summers, voltage controlled voltage source, sine shaper and etc. The elements or blocks must be connected in such a way to emulate real system behavior. The results of this work however, will serve as benchmarks for real analog emulators and as guide during its implementation.

Furthermore, an analog module of constant PQ load model (differential form) was developed using the mathematical equations that express the active and reactive powers at any instant of time as an algebraic function of the load bus magnitude and frequency at that instant (see subsection 2.6.3). Since other types of static load model are also defined relative to the load complex power, further modifications could be made on the proposed PQ-load module to arrive at any other constant load parameter.

LIST OF GRADUATED STUDENTS PARTIALLY OR WHOLLY SUPPORTED BY PROJECT

PH.D.

1. Aaron St. Leger	Ph.D. ECE	Graduated – 6/08
2. Anthony Deese	Ph.D. ECE	Graduated – 6/08
3. Petya Vachrununkiet	Ph.D. ECE	Graduated – 6/07
4. Chris Dafis	Ph.D. ECE	Graduated – 6/05
5. Anawach Sangswang	Ph.D. ECE	Graduated – 6/03

M.Sc

1. Qingyan Liu	M.Sc. ECE	Graduated – 6/05
2. Michael Olaleye	M.Sc. ECE	Graduated – 6/04
3. Bhavana Kashavamurthy	M.Sc. ECE	Graduated – 6/04

LIST PUBLICATIONS SUPPORTED BY PROJECT

JOURNALS:

[1] A. Deese and C. Nwankpa, "Application of Analog and Hybrid Computation Methods to Fast Power System Security Studies", to be published in *International Journal of Electrical Power and Energy Systems*

[2] A. Deese and C. Nwankpa, "Analog Emulation of Power System Load Behavior" *IET Proceedings on Generation, Transmission & Distribution* Volume 3, Issue 6, June 2009 Page(s):535 - 546

[3] A. St. Leger and C. Nwankpa, "OTA Based Transmission Line Model with Variable Parameters for Analog Power Flow Computation" *International Journal of Circuit Theory and Applications*, 2008.

[4] Wang, X, Ziavras, S. Nwankpa, C., Johnson, J., Nagvajara, P. "Parallel solution of Newton's power flow equations on configurable chips", *International Journal of Electric Power & Energy Systems*, Volume 29, Issue 5, June 2007, Pages 422-431.

REFEREED CONFERENCES:

[1] Anthony Deese, Juan C. Jiménez, John Berardino, and Chika O. Nwankpa "Hardware Prototype to Emulate the Dynamics of Power System Generators with Field Programmable Analog Arrays" ISCAS 2010, Paris, France.

[2] J. Jimenez and C. Nwankpa, "Analysis of Reconfigurable Tap Changing Transformer Model Through Analog Emulation," *Proceedings of 2009 International Symposium on Circuits and Systems(ISCAS'09)*, May, 2009, Taiwan.

[3] A. Deese, J. Jimenez and C. Nwankpa, "Utilization of Field Programmable Analog Arrays (FPAA) to Emulate Power System Dynamics." *Proceedings of 2009 International Symposium on Circuits and Systems(ISCAS'09)*, May, 2009, Taiwan.

[4] C. Nwankpa, J. Johnson, P. Nagvajara, T. Chagnon and P. Vachranukunkiet, "FPGA Hardware Results for Power System Computation," *Proceedings of 2009 IEEE Power Systems Conference and Exposition (PSCE'09),* March, 2009, Seattle, WA.Johnson, J.

[5] Chagnon, T, Vachrununkiet, P, Nagvajara, P and Nwankpa, C. "Sparse LU Decomposition using FPGA" Proceedings of *PARA 2008* in Trondheim, Norway, May 13-16, 2008.

[6] C. Nwankpa, J. Johnson, P. Nagvajara, Z. Lin, M. Murach and P. Vachranukunkiet, "Special Purpose Hardware for Power System Computation" Proceedings of 2008 IEEE Power and Energy Society General Meeting, Pittsburg, PA, July 20-24, 2008.

[7] St Leger, A.; Jimenez, J.C.; Agung Fu; Djimbinov, S.; Sa Em Soeurn; Sun Sit Lwin; Nwankpa, C.O.;, "Analog Emulation of a Reconfigurable Tap Changing Transformer", Circuits and Systems, 2007. ISCAS 2007. IEEE International Symposium on 27-30 May 2007 Page(s):73 - 76

[8] Leger, A. St.; Nwankpa, C.O., "Analog and Hybrid Computation Approaches for Static Power Flow System Sciences", 2007. HICSS 2007. 40th Annual Hawaii International Conference on Jan. 2007 Page(s):119 - 119

[9] Nwankpa, C.; Deese, A.; Qingyan Liu; St Leger, A.; Yakaski, J., "Power system on a chip (PSoC)", Circuits and Systems, 2006. ISCAS 2006. Proceedings. 2006 IEEE International Symposium on 21-24 May 2006 Page(s):4 pp.

[10] St Leger, A.; Nwankpa, C.O., "Static generator model for analog power flow computation", Circuits and Systems, 2006. ISCAS 2006. Proceedings. 2006 IEEE International Symposium on 21-24 May 2006 Page(s):4 pp.

[11] Deese, Anthony S.; Leger, Aaron St.; Nwankpa, C.O., "Effect of Size on Analog Circuit Based Emulation of Steady-State Power System Behavior", Circuits and

Systems, 2006. MWSCAS '06. 49th IEEE International Midwest Symposium on Volume 1, 6-9 Aug. 2006 Page(s):581 - 585

[12] Nwankpa, C.; Deese, A.; Qingyan Liu; Leger, A.S.; Yakaski, J.; York, N., "Power system on a chip (PSoC): analog emulation for power system applications", Power Engineering Society General Meeting, 2006. IEEE 18-22 June 2006 Page(s):13 pp.

[13] Murach, M.; Vachranukunkiet, P.; Nagvajara, P.; Johnson, J.; Nwankpa, C., "Optimal reconfigurable HW/SW co-design of load flow and optimal power flow computation", Power Engineering Society General Meeting, 2006. IEEE 18-22 June 2006 Page(s):5 pp.

[14] Deese, A.S.; Nwankpa, C.O., "Emulation of power system load dynamic behavior through reconfigurable analog circuits", Circuits and Systems, 2006. ISCAS 2006. Proceedings. 2006 IEEE International Symposium on 21-24 May 2006 Page(s):4 pp.

[15] Murach, M.; Nagvajara, P.; Johnson, J.; Nwankpa, C., "Optimal power flow utilizing FPGA technology", Power Symposium, 2005. Proceedings of the 37th Annual North American 23-25 Oct. 2005 Page(s):97 - 101

[16] Qingyan Liu; Nwankpa, C.O., "Applications of operational transconductance amplifier in power system analog emulation", Circuits and Systems, 2005. ISCAS 2005. IEEE International Symposium on 23-26 May 2005 Page(s):5302 - 5305 Vol. 5

[17] Carullo, S.P.; Olaleye, M.; Nwankpa, C.O., "VLSI based analog power system emulator for fast contingency analysis", System Sciences, 2004. Proceedings of the 37th Annual Hawaii International Conference on 5-8 Jan. 2004 Page(s):8 pp.

LIST OF REFERENCES

[1] Wolfram Research, Mathematica Applications, Analog Insydes 2.0 http://documents.wolfram.com/applications/insydes/Tutorial/BehavioralModels.html

[2] User's Guide, OrCAD Pspice, Capture CIS version 9.2.3, Cadence Design Systems, Inc. http://cadence.com

[3] C. Clapham, The concise Oxford Dictionary of Mathematics (in Physical Sciences and Mathematics). Oxford University Press, 1996.

[4] Encyclopedia Britannica Online. http://www.search.eb.com/

[5] The Free On-line Dictionary of Computing, http://www.foldoc.org/ , Editor Dennis Howe

[6] P.C. Krause, T.A. Lipo and D.P. Carroll, "Applications of Analog and Hybrid Computation in Electric Power System Analysis," Proceedings of the IEEE, Vol. 62, No. 7, July 1974.

[7] P.G. McLaren, P. Forsyth, A. Perks and P.R. Bishop, "New Simulation Tools for Power Systems", Transmission and Distribution Conference and Exposition, 2001. IEEE/PES, vol. 1, 28, pp. 91-96, Oct-2 Nov, 2001.

[8] A.B. Clymer, "The Mechanical Analog Computers of Hannibal Ford and William Newell," IEEE Annals of the History of Computation, Vol. 15, No. 2, pp. 19-34, 1993.

[9] V. Bush, "The Differential Analyzer: A New Machine for Solving Differential Equations." Journal of the Franklin Institute, vol. 212, no. 4, pp. 447-488, 1931.

[10] J.S. Small, "General-Purpose Electronic Analog Computing: 1945-1965," IEEE Annals of the History of Computation, Vol. 15, No. 2, pp. 8-18, 1993.

[11] A. Greenwood, Electrical Transients in Power Systems. 2nd Edition, John Wiley & Sons, Inc., New York, 1991

[12] R. Joetten, T. Wess, J. Wolters, H. Ring, and B. Bjoernsson, "A new Real-Time Simulator for Power System Studies," IEEE Transactions, Vol. PAS 104, No. 9, pp. 2604-2611, 1985

[13] D. P. Carrol, "Digital and Hybrid Computer Simulation of Power Systems," SIMULATION, July 1973, pp. 9-15.

[14] E.L. Harder and G.D. McCann, "A Large-Scale General-Purpose Electric Analog Computer," AIEE Transactions, Vol. 67, pp.664-673, 1948.

[15] G.A. Korn and T.M. Korn, Electronic Analogue Computers (D-C Analogue Computers), McGraw-Hill, New York, 2nd edition, 1956.

[16] P.D. Jennings and G.E. Quinan, "The Use of Business Machines in Determining the Distribution of Load and Reactive Components in Power Line Networks," AIEE Transactions, Vol. 65, pp. 1045-1046, 1946.

[17] D.F. Shankle, C.M. Murphy, R.W. Long, and E.L. Harder, "Transient-Stability Studies-I-Synchronous and Induction Machines," AIEE Transactions PAS Vol.73, pp. 1563-1580, 1954.

[18] H.W. Dommel, "Digital Computer Solutions of Electromagnetic Transients in Single and Multiphase Networks," IEEE Transactions on PAS, Vol. PAS-88, No. 4, pp. 388-399, April 1969.

[19] G. Nimmersjo, O. Werner-Erichsen, B. Hillstrom, G.D. Rockefeller, "A digitally-controlled, real-time, analog power system simulator for closed-loop protective relay testing," IEEE Transactions on Power Delivery, Vol. 3, No. 1, pp. 138-152, January 1988.

[20] M. Hirakami and W. Neugebauer, "Transient Network Analyzer Operation with Digital Computer Control and Analysis," IEEE Transactions on Power Aparatus and Systems, Vol. PAS-100, No. 4, April 1981

[21] Y. Tamura, E. Dan, I Horie, Y. Nakanishi, and S. Yokokawa, "Development of Power System Simulator for Research and Education," IEEE Transactions on Power Systems, Vol.5, No. 2, pp. 492-498, May 1990.

[22] B. Stott and O. Alsac, "Fast Decoupled Load Flow," IEEE Transactions on Power Apparatus and Systems, Vol. PAS-93, No. 3, pp.859-869, 1974.

[23] M. Crow, Computational Methods for Electric Power Systems. CRC Press, 2003.

[24] R. W. Newcomb and J.D. Lohn, "Analog VLSI for Neural Networks" in Handbook of Brain Theory and Neural Networks, M. Arbib Ed., Bradford Books, MIT Press, 1995.

[25] J.D. Glover and M.S. Sarma, Power System Analysis and Design, Brooks/Cole, CA, 2002.

[26] S. Rahman, "Power for the internet", IEEE Computer Applications in Power, Vol. 14, No. 4, Oct. 2001, pp. 8-10, based on statistics published by the US-Department of Energy.

[27] E.A. Vittoz, "The Design of High-Performance Analog Circuits on Digital CMOS Chips," IEEE Journal of Solid-State Circuits, Vol. SC-20, No. 3, pp. 657-665, June 1985.

[28] R. Fried, R.S. Cherkaoui, C.C. Enz, A. Germond, and E.A. Vittoz, "Approaches for Analog VLSI Simulation of the Transient Stability of Large Power

Networks," IEEE Transactions on Circuits and Systems-I: Fundamental Theory and Applications, Vol. 46, No.10, pp. 1249-1263, October 1999.

[29] S.P. Carullo, M. Olaleye and C.O. Nwankpa, "VLSI Based Analog Power System Emulator for Fast Contingency Analysis", Proceedings of the 37th Hawaii International Conference on System Sciences, pages 60-67, January 2004.

[30] M.B. Olaleye and C.O. Nwankpa, "Analog Behavioral Models for the Purpose of Analog Emulation of Large Scale Power Systems," The Proceedings of the 36th North American Power Symposium (NAPS), pp. 97-104, August 2004.

[31] J. Tabler, M. Brooke, J. Dorsey and S. Arayani, "Solution of Massively Parallel Systems of Nonlinear Equations Using Analog Circuits," Proceedings of the 35th Midwest Symposium on Circuits and Systems, Vol. 1, pp. 764-767, August 1992.

[32] J.R. Ashley, Introduction to Analog Computation. John Wiley and Sons, Inc., New York, 1963.

[33] G. R. Peterson, Basic Analog Computation. The Macmillan Company, New York, 1967.

[34] C.L. Johnson, Analog Computer Techniques, McGraw-Hill Book Company, Inc., New York, 1963.

[35] P.M. Anderson and A.A. Fouad, Power System Control and Stability. IEEE Press, New York, 1994.

[36] J.J. Grainger and W.D. Stevenson, Jr., Power System Analysis, McGraw-Hill, Inc., New York, NY, 1994.

[37] P. Kundur, Power System Stability and Control, McGraw-Hill, Inc., New York, NY, 1994.

[38] H.E. Brown, Solution of Large Networks by Matrix Methods. John Wiley & Sons, Inc., New York, NY, 1985.

[39] H. Saadat, Power System Analysis, McGraw-Hill Primis Custom Publishing, 2002.

[40] C. Concordia and S. Ihara, "Load Representation in Power System Stability Studies", IEEE Transactions on Power Apparatus and Systems, Vol. PAS-101, No. 4, April 1982.

[41] IEEE Task Force on Load Representation for Dynamic Performance, "Load Representation For Dynamic Performance Analysis", IEEE Transactions on Power Systems, Vol. 8, No. 2, May 1993.

[42] PowerWorld Simulator v.9.1, PowerWorld Corporation, Champaign IL. http://www.powerworld.com

[43] Power System Simulator for Engineering (PSS/E)-28.1.4, Power Technologies, Inc. http://www.shawgrp.com/PTI/software/psse/

[44] Capture CIS version 9.2.3, Cadence Design Systems, Inc. http://cadence.com

[45] C.O. Nwankpa, "Stochastic Models for Power System Dynamic Stability Analysis", Ph.D. Report, Illinois Institute of Technology, Chicago, IL., 1990.

[46] B.C. Lesieutre, P.W. Sauer and M.A. Pai, "Development and Comparative Study of Induction Machine Based Dynamics P, Q Load Models", IEEE Transactions on Power Systems, Vol. 10, No. 1, February 1995.

[47] B. Gilbert, "A monolithic Microsystem for Analog Synreport of Trigonometric Functions and Their Inverses", IEEE Journal of Solid State Circuits, Vol. SC-17, No. 6, pp. 1179-1191, December 1982.

[48] S. Prigozy, "Novel Applications of SPICE in Engineering Education", IEEE Transactions on Education, Vol. 32, No. 1, pp.35-38, February 1989.

[49] L. Hedger, "ANALOG COMPUTATION: Everything Old Is New Again", Indiana University, Research & Creative Activity, Volume XXI, Number 2, April 1998. http://www.indiana.edu/~rcapub/v21n2/p24.html

APPENDIX A. POWER SYSTEM TEST SAMPLES WITH PARAMETERS

This section provides other samples of power system sizes and parameters used in the validation of analog emulator module developed using Analog Behavioral Models and analog devices in PSpice design environment.

A.1 6-Bus Power System (3 generators, 8 lines and 3 loads)

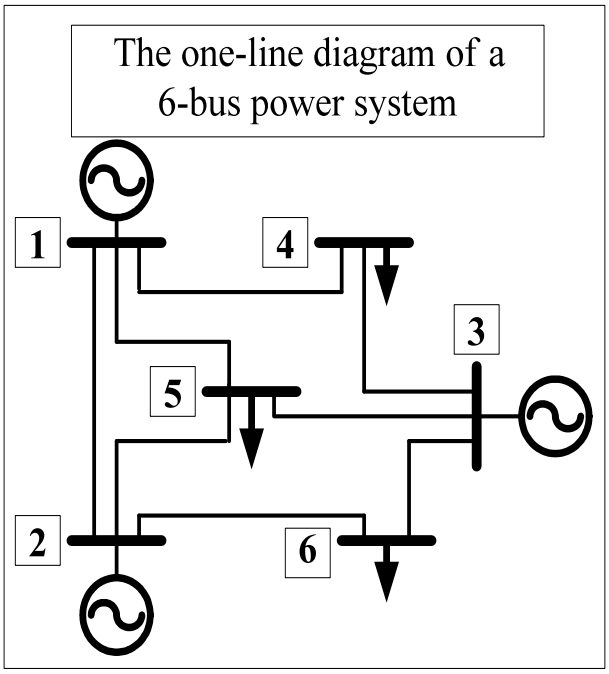

Figure A.1: Sample 6-Bus Power System

Table A.1: System Parameters for Sample 6-Bus Power System

Bus Data (pu)						Line Data (pu)	
Bus #	$\lvert V \rvert$	P	Q	H	D		
Bus 1	1.04	-	-	-	-	R_{12}	0.020
						X_{12}	0.115
Bus 2	1.01	0.7	-	4s	-	R_{14}	0.035
						X_{14}	0.225
Bus 3	1.03	1.0	-	5s	-	R_{15}	0.025
						X_{15}	0.105
Bus 4	-	1.0	0.35	-	-	R_{25}	0.025
						X_{25}	0.105
Bus 5	-	1.5	0.50	-	-	R_{26}	0.028
						X_{26}	0.125
Bus 6	-	1.0	0.25	-	-	R_{34}	0.215
						X_{34}	0.215
						R_{35}	0.035
						X_{35}	0.215
						R_{36}	0.026
						X_{36}	0.175

A2 14-Bus Power System (5 generators, 21 lines and 9 loads)

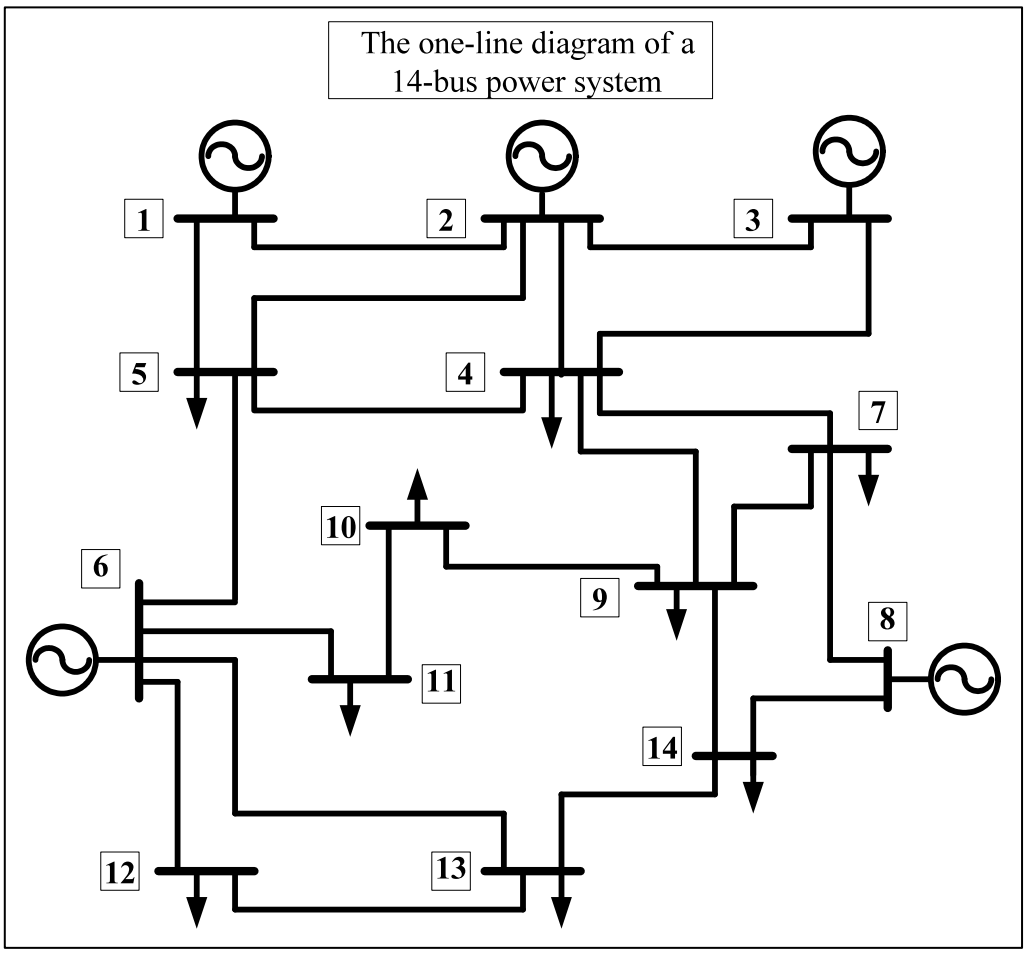

Figure A.2: Sample 14-Bus Power System

Table A.2: System Parameters for Sample 14-Bus Power System

Bus Data (pu)						Line Data (pu)	
Bus #	$\|V\|$	P	Q	H	D		
Bus1	1.0	-	-	-	-	X_{12}	0.05917
Bus 2	1.0	0.3	-	4s	-	X_{15}	0.22304
Bus 3	1.0	0.4	-	5s	-	X_{23}	0.03297
Bus 4	-	0.478	0.39	-	-	X_{24}	0.17632
Bus 5	-	0.18	0.05	-	-	X_{25}	0.17388
Bus 6	1.0	0.4	-	5s	-	X_{34}	0.37103
Bus 7	-	0.2	0.05	-	-	X_{45}	0.04211
Bus 8	1.0	0.5	-	5.4s	-	X_{47}	0.20450
Bus 9	-	0.3	0.1	-	-	X_{49}	0.53890
Bus 10	-	0.19	0.02	-	-	X_{56}	0.23490
Bus 11	-	0.14	0.02	-	-	X_{611}	0.19890
Bus 12	-	0.16	0.03	-	-	X_{612}	0.25581
Bus 13	-	0.34	0.05	-	-	X_{613}	0.63027
Bus 14	-	0.3	0.05	-	-	X_{78}	0.17615
						X_{79}	0.11001
						X_{814}	0.21300
						X_{910}	0.08450
						X_{914}	0.01270
						X_{1011}	0.19207
						X_{1213}	0.05988
						X_{1314}	0.34802

APPENDIX B. PSPICE CIRCUITS

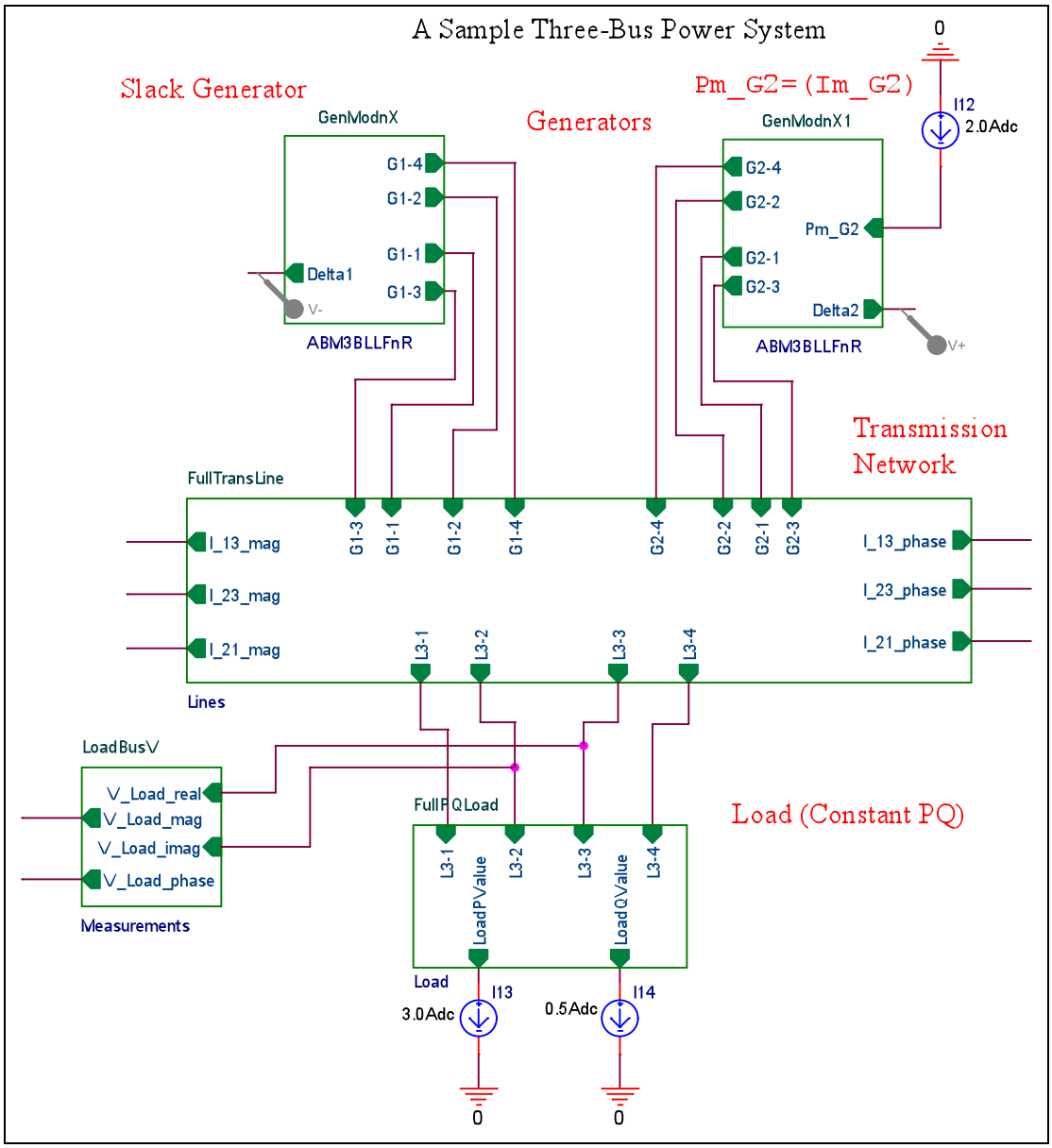

Figure B.1: Hierarchical Block of a Sample 3-Bus Power System

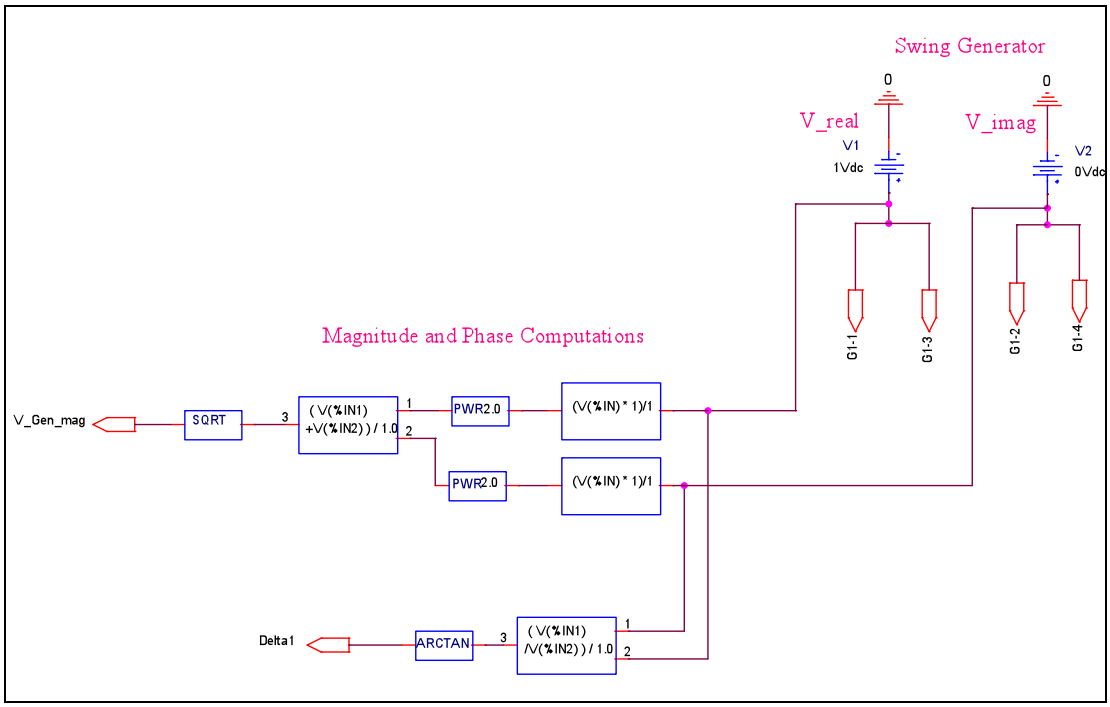

Figure B.2: PSpice Circuit Representation of a Swing Generator

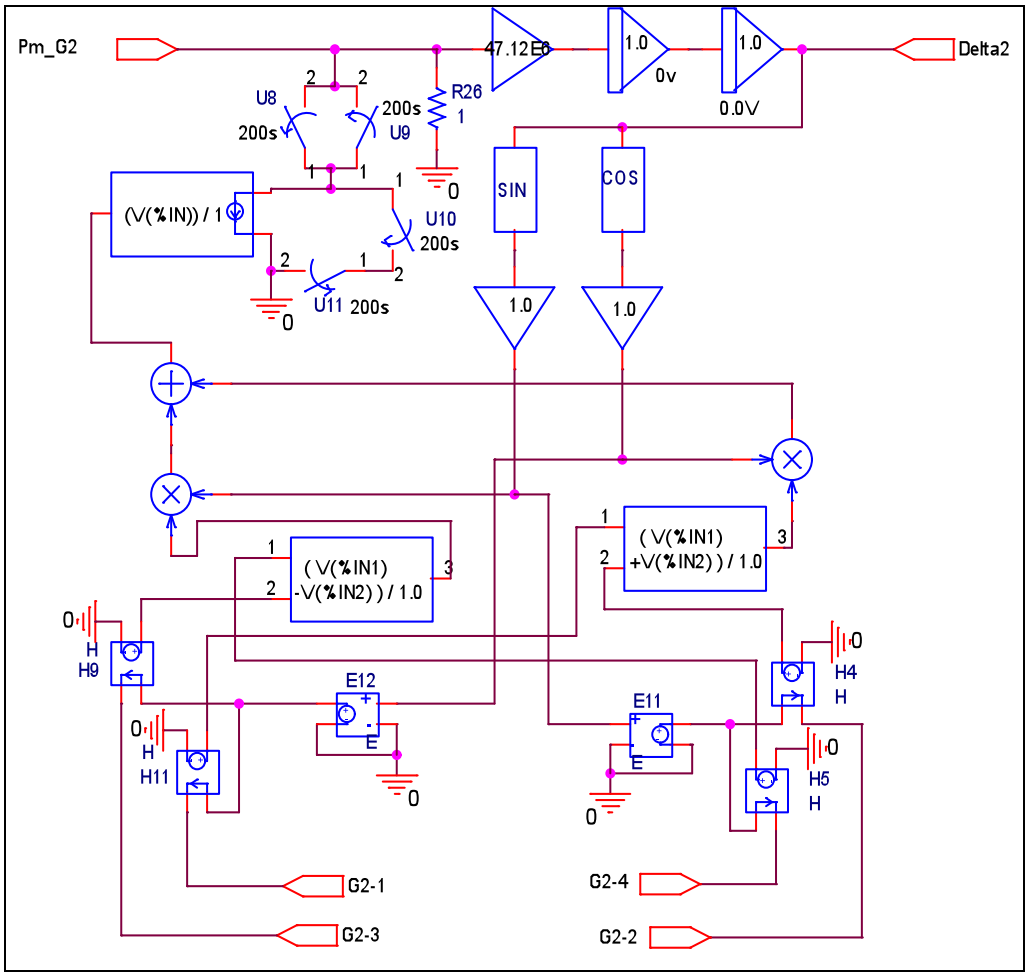

Figure B.3: PSpice Circuit Representation of a Generator Module

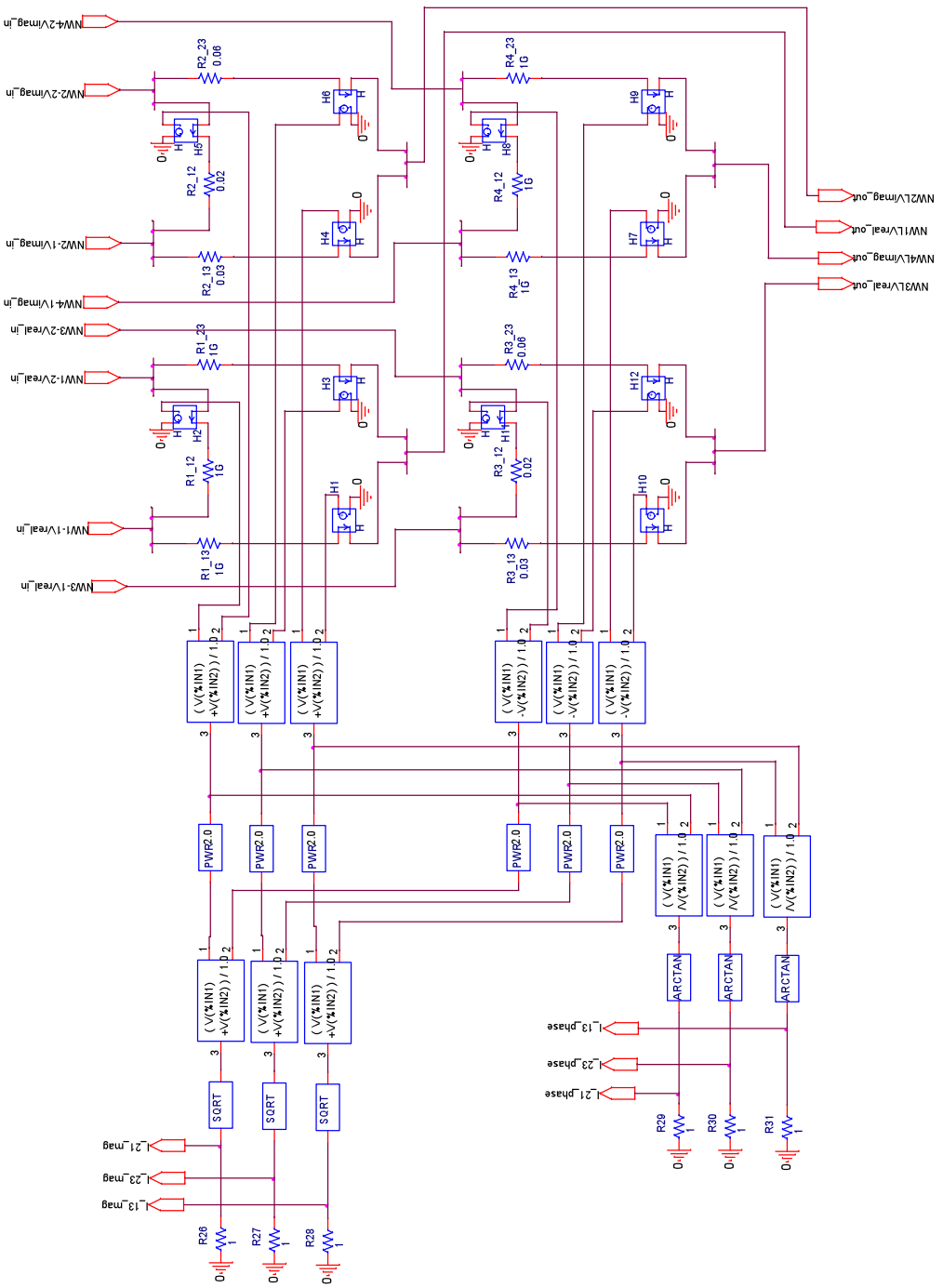

Figure B.4: PSpice Circuit Representation of Transmission Networks (3-Bus Power System Sample)

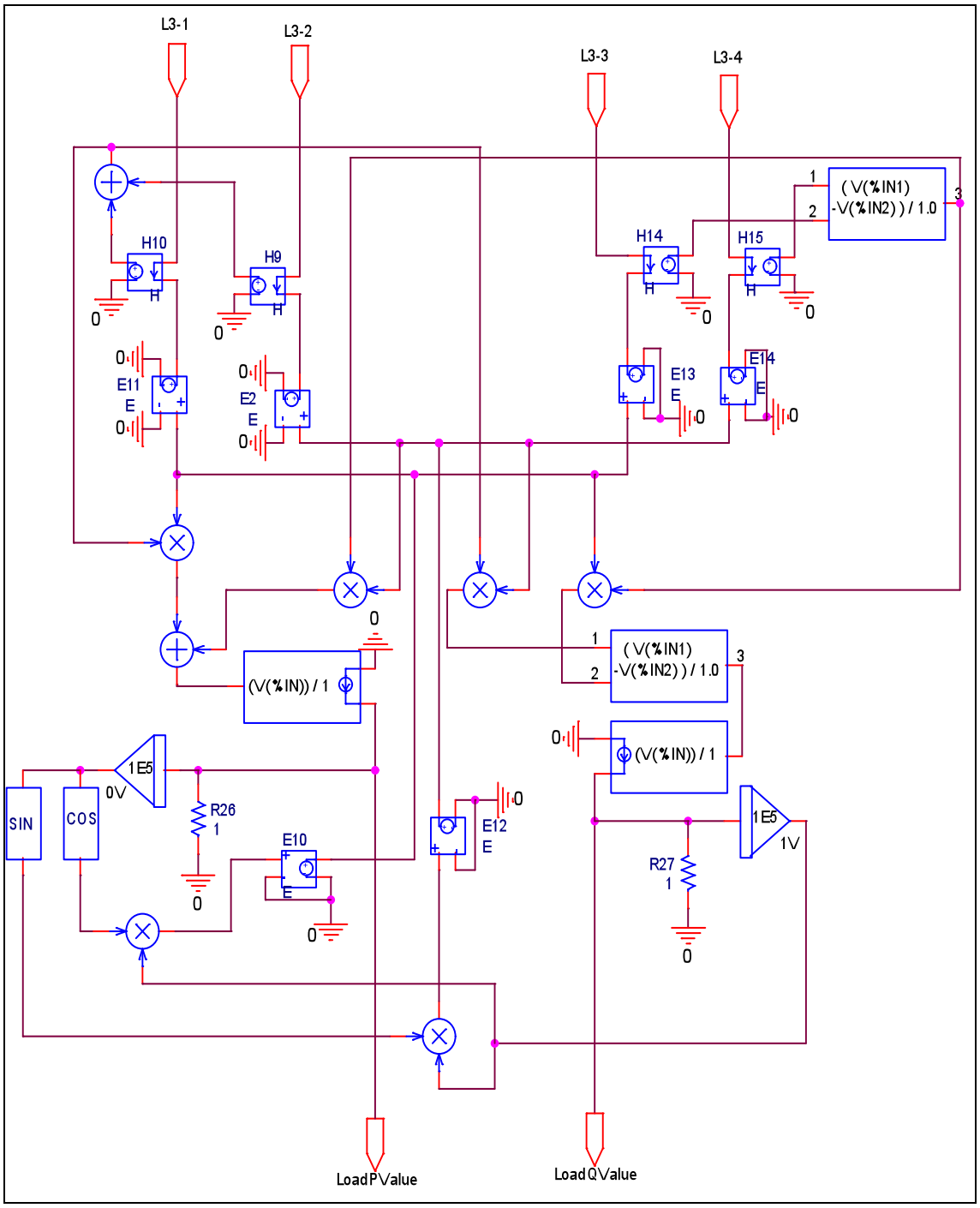

Figure B.5: PSpice Circuit Representation of Constant PQ-Load (Differential Form)

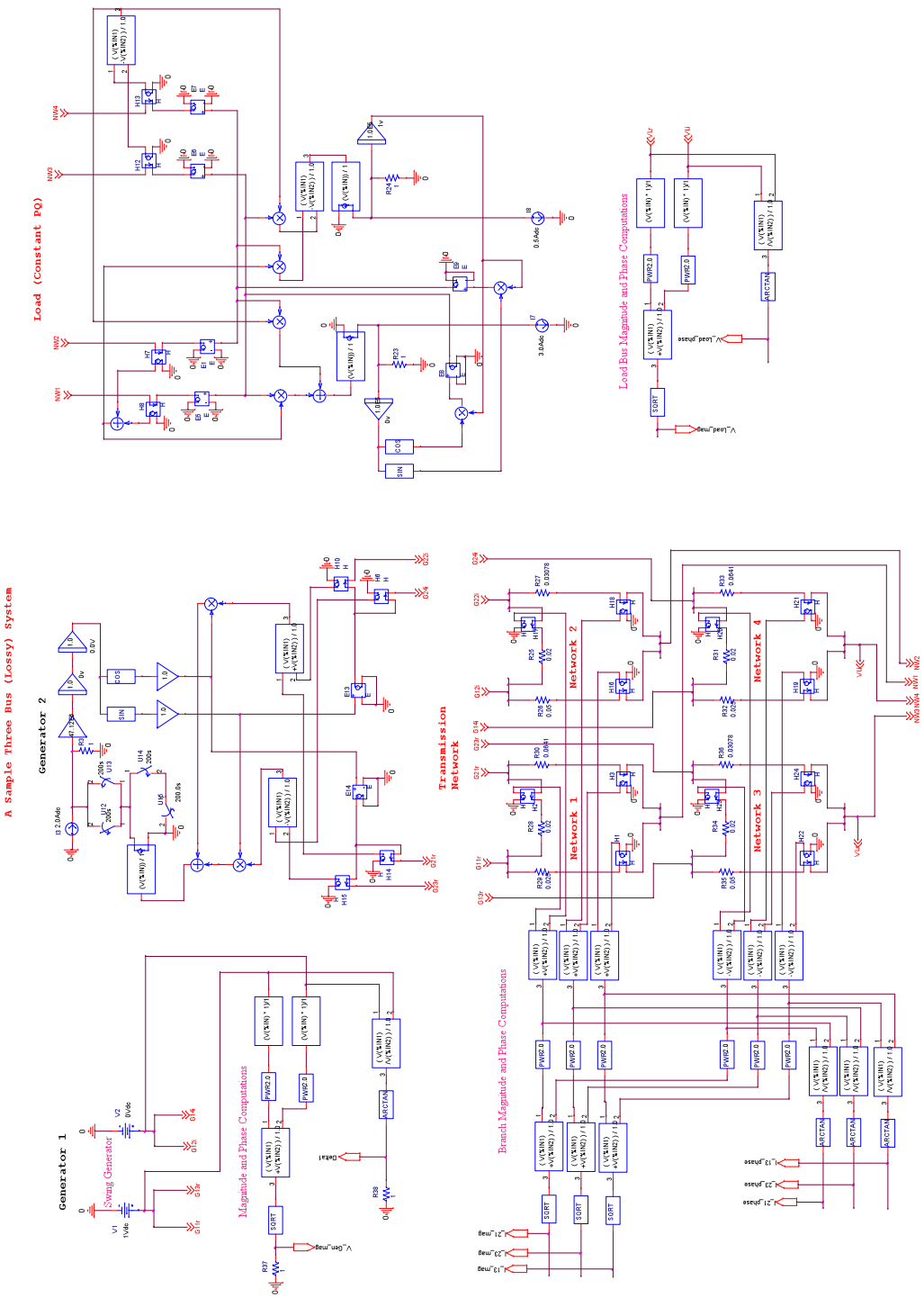

Figure B.6: PSpice Circuit Representation of a 3-Bus Power System

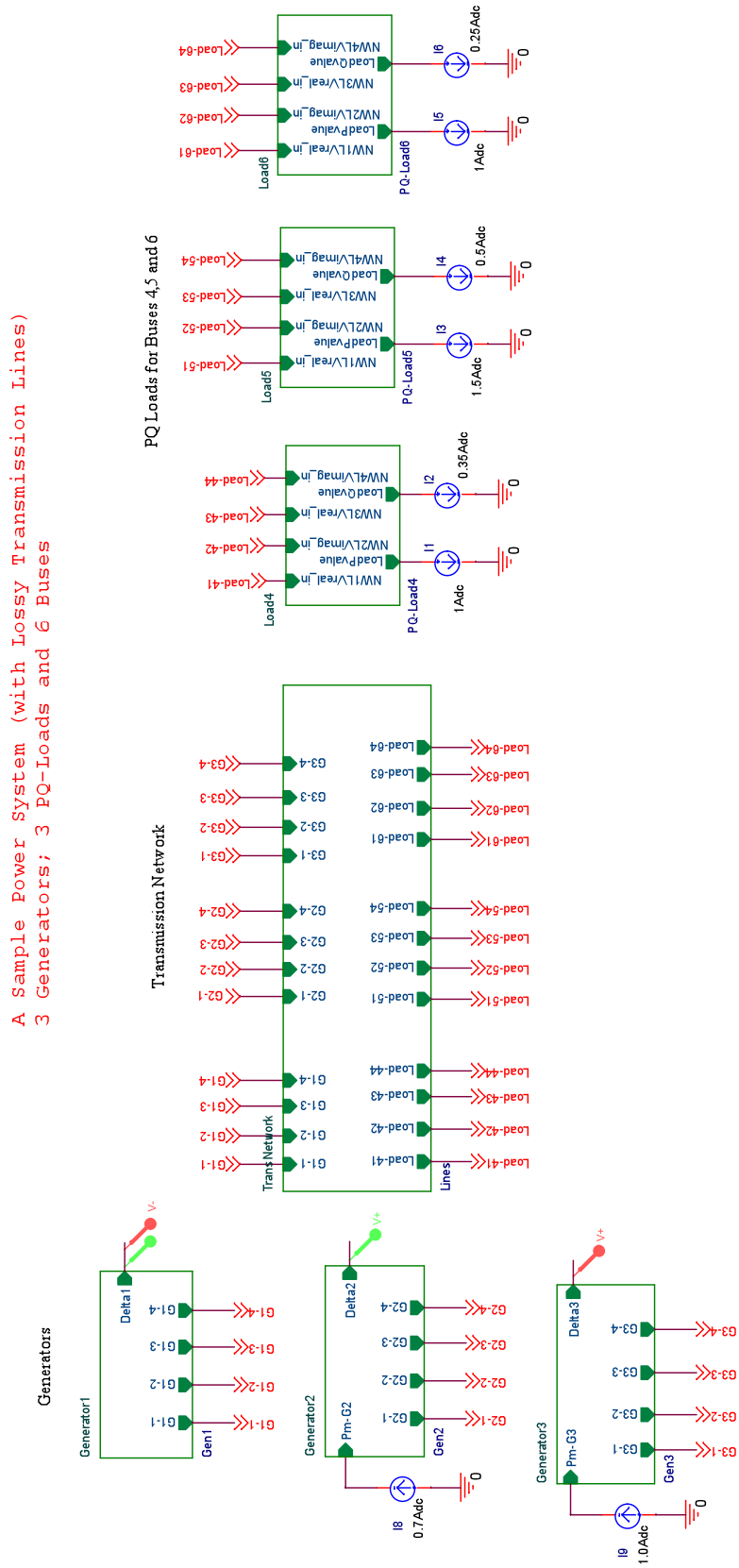

Figure B.7: PSpice Circuit Representation of a Sample 6-Bus Power System (Hierarchical Block Form)

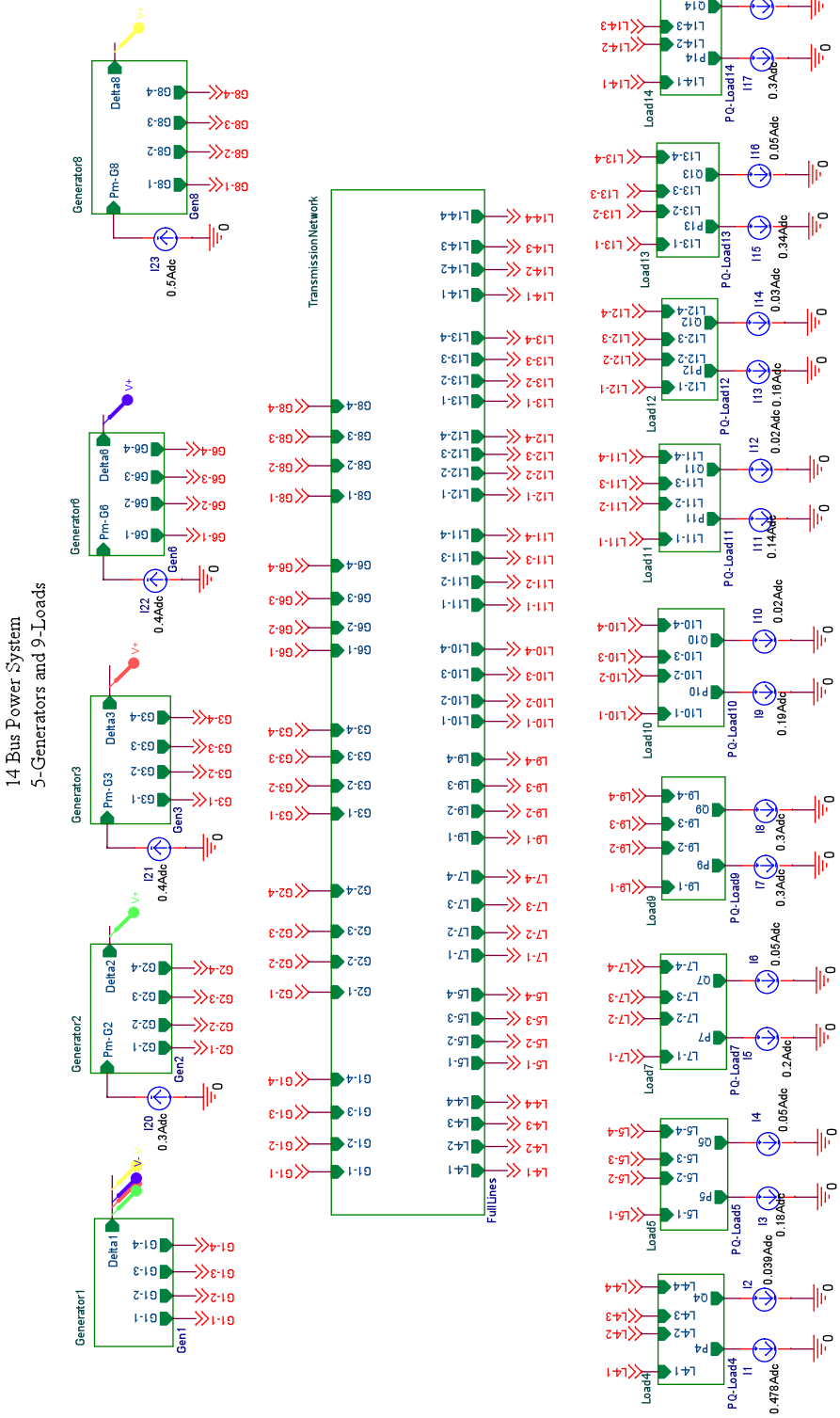

Figure B.8: PSpice Circuit Representation of a Sample 14-Bus Power System (Hierarchical Block Form)